

N 71 12810

NASA CR-72764

ORNL-4608

UC-25 – Metals, Ceramics, and Materials

CASE FILE
COPY

SYNTHESIS, CHARACTERIZATION, AND
FABRICATION OF UN

by

V. J. Tennery, T. G. Godfrey, and R. A. Potter

OAK RIDGE NATIONAL LABORATORY

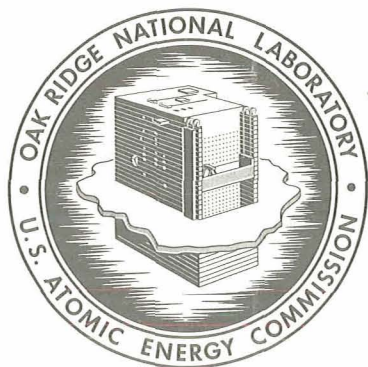
prepared for

NATIONAL AERONAUTICS AND
SPACE ADMINISTRATION

NASA Lewis Research Center

Contract C-51092-B

Robert R. Metroka, Project Manager



OAK RIDGE NATIONAL LABORATORY

operated by

UNION CARBIDE CORPORATION

for the

U.S. ATOMIC ENERGY COMMISSION

Printed in the United States of America. Available from
National Technical Information Service
U.S. Department of Commerce, Springfield, Virginia 22151
Price: Printed Copy \$3.00; Microfiche \$0.65

This report was prepared as an account of work sponsored by the United States Government. Neither the United States nor the United States Atomic Energy Commission, nor any of their employees, nor any of their contractors, subcontractors, or their employees, makes any warranty, express or implied, or assumes any legal liability or responsibility for the accuracy, completeness or usefulness of any information, apparatus, product or process disclosed, or represents that its use would not infringe privately owned rights.

NASA CR-72764
ORNL-4608

TOPICAL REPORT

SYNTHESIS, CHARACTERIZATION, AND FABRICATION OF UN

by

V. J. Tennery, T. G. Godfrey, and R. A. Potter

OAK RIDGE NATIONAL LABORATORY
operated by
Union Carbide Corporation
Nuclear Division
Post Office Box X
Oak Ridge, Tennessee 37830

prepared for

NATIONAL AERONAUTICS AND SPACE ADMINISTRATION

DECEMBER 1970

CONTRACT C-51092-B

NASA Lewis Research Center
Cleveland, Ohio
Robert R. Metroka, Project Manager

CONTENTS

	<u>Page</u>
Abstract	1
Introduction	1
Synthesis of Uranium Nitride Powders	3
Determination of the Distribution of Particle Sizes in Uranium Nitride Powders	8
The Morphology of Uranium Nitride Particles.	13
Fabrication of Uranium Nitride	17
Quantitative Chemical Analysis of UN	27
Sintering of UN	42
Thermal Stability of UN	44
Machining Study of UN	52
UN Specimens Delivered to the Lewis Research Center of the National Aeronautics and Space Administration	58
Conclusions	60
Acknowledgments	62

SYNTHESIS, CHARACTERIZATION, AND FABRICATION OF UN

V. J. Tennery, T. G. Godfrey, and R. A. Potter

ABSTRACT

We developed procedures for synthesizing fine uranium nitride powders that contain less than 200 ppm O from uranium metal by the hydride-dehydride-nitride process. We established a method based on the principle of gas sedimentation as suitable for measuring the distribution of particle sizes and found that 80% of the particles were between 1 and 7 μm in diameter. Scanning electron microscopy showed that the particles were very irregularly shaped and that each particle had several protrusions from the surface, which explains the difficulty in fabricating these powders.

We fabricated uranium mononitride (UN) cylinders by both uniaxial and isostatic pressing. Uniaxial pressing required additives such as camphor to act as a binder and die lubricant, but the addition of camphor resulted in about 1000 ppm O in the sintered product. Isostatic pressing required no additives and typically resulted in a sintered product with less than 300 ppm O.

We found that the precision and accuracy possible in the analyses for uranium and nitrogen were the limiting factors for adequate quantitative chemical analysis of UN. We found that the microstructure of UN bodies of about 85% theoretical density was very stable when subjected to 1400°C (1673 K) for 100 hr in vacuum; very small shrinkages of about 1/2 to 1% were accompanied by very small increases in grain size.

Conventional grinding of UN produced minute cracks in the machined surface, but electrodischarge machining produced very smooth surfaces with a thin coating of an unidentified phase.

INTRODUCTION

The high density of fissile atoms, high melting point, high thermal conductivity, and cubic crystal structure of uranium mononitride (UN) make it a promising nuclear fuel for liquid-metal-cooled reactors. The phase stability of the compound is satisfactory at the temperatures contemplated for use in these reactors, and its chemical compatibility with

lithium and other potential alkali-metal coolants, compared to that of the oxide or carbide, is also a major advantage.^{1,2}

The uranium nitrides UN and uranium sesquinitride (U_2N_3) have been identified and their crystal structures known for some time.^{3,4} Uranium mononitride has a face-centered cubic crystal structure of the NaCl type with a lattice parameter of 4.889 ± 0.001 Å and a theoretical density of 14.32 g/cm^3 . Uranium sesquinitride can be indexed assuming a body-centered cubic crystal structure of the MnO_3 type with a lattice parameter of 10.678 ± 0.005 Å. The x-ray density is 11.24 g/cm^3 . A hexagonal form of this compound has been reported⁵ and is apparently a nitrogen deficient form of U_2N_3 which can be described as UN_x , where x is between 1.33 and 1.50. Another compound, UN_2 , has been reported by Rundle⁶ but really may be UN_x with x less than 1.82 (ref. 5).

The sesquinitride is not a potential fuel in sintered form, because it tends to dissociate at high temperatures into UN and nitrogen gas and because inordinately high nitrogen pressures would be required to achieve appreciable sintering while maintaining the phase intact. Its low density as compared to UN also makes it unattractive.

Fabrication of dense sintered fuel pellets of UN is difficult because the nitride powders react rapidly and exothermally with oxygen and thus are easily contaminated, because the nitride powders cannot be easily compacted by conventional techniques of uniaxial pressing, and because the fabricated parts must be sintered above 2000°C (2273 K) in

¹E. O. Speidel and D. L. Keller, Fabrication and Properties of Hot-Pressed Uranium Mononitride, BMI-1633 (May 1963).

²J. Bugl and D. L. Keller, Nucleonics 9, 66-70 (1964).

³J. Bugl and A. A. Bauer, J. Am. Ceram. Soc. 47(9), 425-429 (1964).

⁴J. J. Katz and Eugene Rabinowitch, Chemistry of Uranium, Part I, pp. 232-241, McGraw-Hill, New York, 1951.

⁵A. Naoumidis, Investigations of Uranium Nitrides and Carbonitrides, ORNL-tr-1918, Reports of the Jülich Nuclear Research Center, JUL-472-RW (March 1967).

⁶R. E. Rundle et al., J. Am. Chem. Soc. 70, 99 (1948).

a high-purity nitrogen atmosphere if densities of the order of 90% of theoretical are to be achieved. After it has been sintered, however, the polycrystalline UN is relatively stable in air and may be machined by conventional methods.

Like the sesquinitride, UN also tends to dissociate at high temperatures (in this case, into uranium and nitrogen), but at 1400°C (1673 K) the nitrogen equilibrium pressure for dissociation is only 8.3×10^{-10} atm (8.4×10^{-5} N/m²). The pressures for dissociation at nominal reactor design temperatures are thus quite low, since at 1400°C (1673 K), for example, the nitrogen pressure within the fuel pin would have to be maintained below 8.3×10^{-10} atm (8.4×10^{-5} N/m²) in order for dissociation to occur continuously within the fuel.

The main purposes of the present work were to determine the characteristics of the uranium nitride powders made by a particular process and the methods required to produce these powders with very low oxygen and carbon contents. Other objectives were (1) to establish if relatively large shapes, such as annular cylinders, could be precisely fabricated while maintaining high purity, (2) to study the sintering characteristics of fabricated parts, and (3) to identify the problems of quantitative chemical analysis of sintered UN.

SYNTHESIS OF URANIUM NITRIDE POWDERS

The uranium nitride powders used in this program were produced by the hydride-dehydride-nitride process from starting material of uranium metal, either in bar or plate form. Great care had to be exercised in designing and operating the equipment for synthesizing the powders in order to minimize contamination by oxygen and metallic elements.

The surface of the metal was thoroughly cleaned of all oxides by immersing the metal in a 1 N solution of nitric acid. After the oxide contaminants were removed, the uranium metal was washed with absolute ethanol several times and then stored under ethanol until it was transferred into the inert-atmosphere glove box for loading into the synthesis chamber. The uranium metal was removed from the ethanol bath that protected it from oxidation and quickly inserted into the vacuum vestibule

of the glove box. The pressure in this vestibule was reduced to about 4×10^{-4} torr (5.33×10^{-2} N/m²) within 10 min by means of a mechanical pump. The vestibule was then backfilled to atmospheric pressure with high-purity argon, and the metal was transferred into the glove box. The argon atmosphere in the glove box was purified by means of a purifier that circulated the gas at about 3 cfm (14.2×10^{-4} m³/sec). The oxygen and moisture levels within the glove box were constantly monitored and were typically 2 ppm O and less than 1 ppm water vapor.

The cleaned metal was placed on the tungsten grate rods of the boat in the reaction chamber. This boat, a cylindrical Inconel container that fit within the reaction chamber, was provided with a series of grate rods placed longitudinally along its entire length. The grate rods supported the massive uranium pieces in such a way that the hydrogen used to fragment the metal could easily contact most of the surface of the bulk uranium. This arrangement greatly improved the kinetics of the hydriding reaction to be described later and thereby shortened this part of the synthesis process. No eutectic reaction of the tungsten grate rods with uranium has ever been observed in the equipment. Grate rods made of stainless steel or Inconel form eutectics at low enough temperatures that there have been instances in which reactions between the uranium and grate rods have been observed during the nitriding process.

The massive uranium was fragmented and reduced to a small particle size via Reaction (1):



Under a pressure of 760 torr (1.01×10^5 N/m²) of hydrogen, Reaction (1) proceeds to the right with reasonable speed for massive uranium at 200 to 250°C (473.15 to 523.15 K). The formation of the hydride causes a localized decrease in density within the uranium and thus causes swelling and fragmentation. At the same hydrogen pressure, heating the UH₃ product to 300 to 350°C (573.15 to 623.15 K) causes Reaction (1) to proceed to the left, and finely divided uranium is the product. The number of hydride-dehydride cycles used in the synthesis must be sufficient to fragment all of the massive uranium in a given charge, which is typically 0.7 to 1.5 kg. We observed that some portions

of the uranium biscuits can only be hydrided with difficulty, although we have been unable to establish any correlation between this behavior and gross or trace impurities. To assure optimum hydriding, we use six hydride-dehydride cycles.

The basic equipment (Fig. 1) consists of a vacuum-tight reaction chamber that can be loaded with clean metal under an inert atmosphere in a glove box. The reaction chamber is then valved off from the atmosphere, transferred out of the glove box, and attached to the equipment. The reaction chamber can be evacuated to 10^{-6} torr (1.33×10^{-4} N/m²) or can be pressurized to any desired pressure to about 1070 torr (1.36×10^5 N/m²) with hydrogen, argon, or nitrogen gas. The purity of the incoming gases was monitored constantly for oxygen by means of a trace oxygen analyzer, as shown in Fig. 1. Oxygen was removed from the hydrogen by passing the gas over hot uranium; the argon and nitrogen were purified by passing these gases over hot chips of Nb-1% Zr alloy. The gases admitted to the reaction chamber typically contained less than 1 ppm O₂ and 10 ppm water vapor. Water vapor was removed from the gases by passing them through columns of molecular sieve and Drierite before they were passed through the oxygen getters.

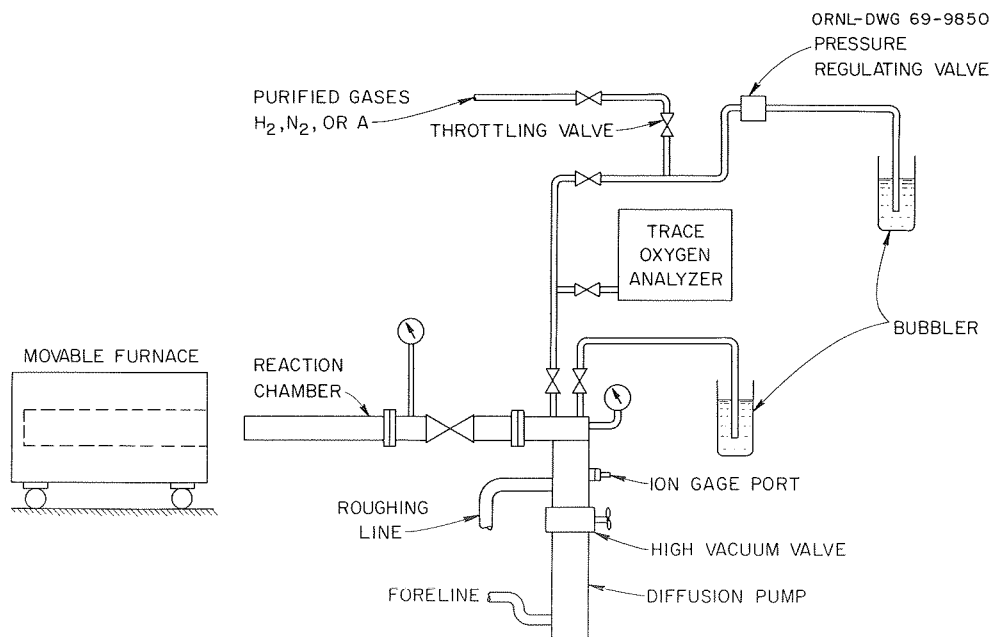


Fig. 1. Schematic Diagram of Apparatus for Synthesis of Uranium Nitride Powder.

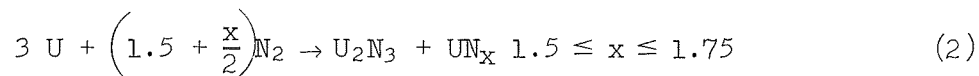
The temperature within the reaction chamber was varied by moving the furnace shown in Fig. 1 over the reaction chamber. The temperature within the chamber was measured by means of a Chromel-P vs Alumel thermocouple whose hot junction was seated inside a well in the reaction chamber. The pressure-regulating valve maintained the system at some arbitrarily designated value above atmospheric pressure during those synthesis steps involving hydriding or dehydriding and during the bulk of the nitriding process.

One hydride-dehydride cycle consisted of the following steps. Hydrogen was introduced into the reaction chamber after the uranium was preheated to about 200°C (473 K). The rate of the reaction was determined qualitatively by observing the rate at which hydrogen gas had to be delivered to the metal to maintain the desired pressure within the system. When the reaction rate had slowed markedly (usually after about 10 to 15 min for about 1 kg of metal) the furnace was moved over the reaction chamber, and the temperature of the charge was increased to about 300°C (573.15 K). In this temperature range the hydrogen pressure over UH_3 would begin to exceed the setting of the pressure-regulating valve, and hydrogen would be released from the system as the UH_3 decomposed. We increased the temperature sufficiently to decompose a large fraction of the UH_3 .

The next cycle would be started by simply rolling the movable furnace off the reaction chamber and thus letting the temperature of the reaction chamber decrease. As the temperature of the charge approached 250°C (523.15 K) the reaction with hydrogen would occur quite rapidly if the uranium had already been processed through at least one hydride cycle.

After the six cycles had been completed, the charge was left in the form of the hydride. The atmosphere in the equipment was changed to nitrogen, and the temperature of the charge increased to about 300°C (573.15 K), for only 2 to 4 min to decompose only a small portion of the UH_3 . The temperature was then decreased, and the small amount of free uranium produced by the preceding high-temperature traverse reacted vigorously with the nitrogen according to Reaction (2). We continued to cycle the temperature, increasing the maximum temperature of each traverse about 15 degrees above the preceding one. In this fashion, only a small

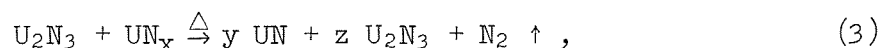
portion of the uranium was nitrided during each cycle. This process greatly reduced the problems associated with the large exothermic



heat observed when nitrogen reacts with uranium.

Continued reaction of nitrogen with the sesquinitride phase, U_2N_3 , led to a solid solution of nitrogen in the U_2N_3 until the compositional parameter x in UN_x approached about 1.6 in the equipment used. The solution of nitrogen in U_2N_3 was strongly dependent upon both temperature and nitrogen pressure. Because of the unavoidable temperature gradient that exists in the reaction chamber, materials having compositions varying from U_2N_3 ($\text{UN}_{1.5}$) to $\text{UN}_{1.6}$ typically were formed within a given batch of powder.

The sesquinitride and nitrogen-rich sesquinitride were heat treated under vacuum to decompose these phases and to transform the powder into a mixture of UN and U_2N_3 according to Reaction (3):



where

$$z \simeq 0.05 \rightarrow 0.2,$$

$$(y + 2z) = 3,$$

$$(y + 3z + 2) = 3 + x.$$

Typically, about 5 to 20% of the powder produced consisted of sesquinitride. Reaction (3) was conducted at 900°C (1173.15 K) under vacuum until the pressure was no higher than 10^{-4} torr (1.33×10^{-2} N/m²). Heat treating at higher temperatures tended to lower sintering activity, and reducing the nitrogen overpressure below the stated value required inordinately long pumping times. After completion of this denitriding step, the reaction chamber was valved off from the system, cooled to room temperature, disconnected from the equipment, and transferred to the inert-atmosphere glove box. The portion of the batch that was located in the hotter regions of the reaction chamber consisted of a very fine gray-bronze mononitride powder. The portion of the powder

that was in the cooler region of the reaction chamber consisted of a very black and fine sesquinitride powder. The powder was passed through a 200-mesh screen, usually without difficulty. The powders were always stored in the glove box in fruit jars tightly sealed by means of a rubber gasket. Bottles sealed with paper or plastic gaskets were not adequate for storing these powders and simultaneously inhibiting contamination by oxygen.

DETERMINATION OF THE DISTRIBUTION OF PARTICLE SIZES IN URANIUM NITRIDE POWDERS

Several experiments were conducted to establish a method for measuring the distribution of particle sizes in the synthesized powders. The uranium nitride powders were strongly pyrophoric, and this greatly increased the difficulty of preparing the powders for analysis. For determination of particle sizes, we considered only those measuring techniques that permitted atmospheric protection for the particles. The methods which were studied were corroborated by means of counting with an optical microscope at 700X. Two measuring methods that did not require extensive new instrumentation appeared to be adaptable to the measurement of nitrides. The Micromerograph (Sharples Corporation, Research Laboratory, Bridgeport, Pennsylvania) and the Coulter Counter (Coulter Electronics, Industrial Division, Hialeah, Florida) both are available commercially and have been used for measuring the distributions of particle sizes in other high-density powders. The Micromerograph operates on the principle of gas sedimentation, and for uranium nitride powders we filled the settling column with very pure nitrogen. The particles were dispersed into the top of the column, which is about 7 ft (2.13 m) high, and settled by gravity onto the pan of a sensitive recording balance located at the bottom of the column. The controlled variable in this measurement was the average density of the particles, which we measured by a toluene immersion technique. Another possible adjustable variable with this instrument would be the gas pressure used to disperse the particles into the top of the column, but, as discussed later, the distribution curve obtained for particle sizes of the uranium

nitride was not really dependent upon the dispersion pressure over the pressure range investigated.

The Coulter Counter operates on the principle of measuring the change in the electrical conductivity across a precisely sized orifice in a suspension of a conducting liquid and the particles to be measured. This technique would be adaptable to a glove-box operation, since the cell that contains the sample can be located remotely from the electronic instrumentation. Aqueous saline liquids are often used with this instrument for measurements on oxide particles, and two of the basic assumptions required with the use of this instrument are that there be no reaction between the particles and the liquid and that the particles not agglomerate in the liquid. As will be discussed, the latter assumptions could not be made for uranium nitride particles.

The results obtained on samples of powder 18 are shown in Fig. 2. The powder sample counted under the optical microscope was suspended in immersion oil to protect it from oxidation. As can be seen in Fig. 2,

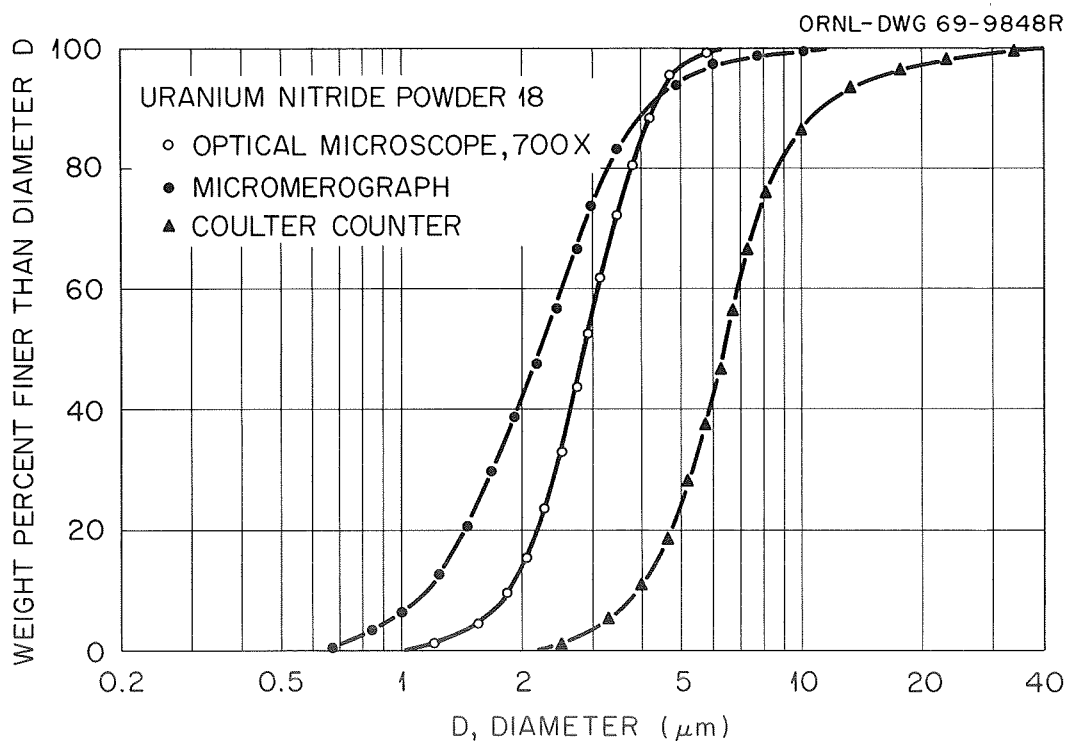


Fig. 2. Distribution of Particle Sizes Obtained by Three Different Methods for a Uranium Nitride Powder.

the data from the optical microscope and Micromerograph agree well at the coarser end of the distribution and diverge from each other somewhat at the small end of the size range, probably because the resolution available with the optical microscope is somewhat limited at sizes below 2 μm . The Coulter Counter, on the other hand, indicated a coarser distribution, and this result is typical when particle agglomeration occurs within the cell electrolyte. This type of result was obtained on several different batches of uranium nitride powder. Organic and inorganic liquids such as isopropyl alcohol and aqueous saline solutions were investigated with the Coulter Counter without reducing the tendency of the particles to agglomerate.

The dependence of the distribution curve upon the dispersion pressure in the Micromerograph was determined between 100 and 300 psi (6.9 and $20.7 \times 10^5 \text{ N/m}^2$). Typical results are shown in Fig. 3 for the powder UN-5. We observed no appreciable dependence of the curve upon dispersion pressure. A typical dependence upon dispersion pressure is one in which the distribution indicates finer particles with increasing pressure, either because of the breakup of agglomerates or the fracturing of individual particles. Neither apparently occurred with the uranium nitride powders investigated.

The curves for distribution of the particle sizes of several different nitride powders were measured with the Micromerograph, and some of these are shown in Fig. 4. The distribution curves for these powders were very reproducible from batch to batch, and, in fact, it was difficult to produce powders that had significantly different distributions by our synthesis process. The specific surface areas of these powders as determined by the Brunauer-Emmet-Teller (BET) method were 0.2 to 0.5 m^2/g .

Some experiments were performed to determine if the curves for distribution of particle sizes of these powders could be shifted to larger sizes by decreasing the number of hydride-dehydride cycles used to fragment the uranium metal. An experimental facility was constructed in which about 10 g of uranium metal could be transformed to the nitride while being observed visually. The temperatures and pressures used were the same as those noted previously. A nitride powder (X-4) was produced in which three hydride-dehydride cycles were used, and another (X-5) was

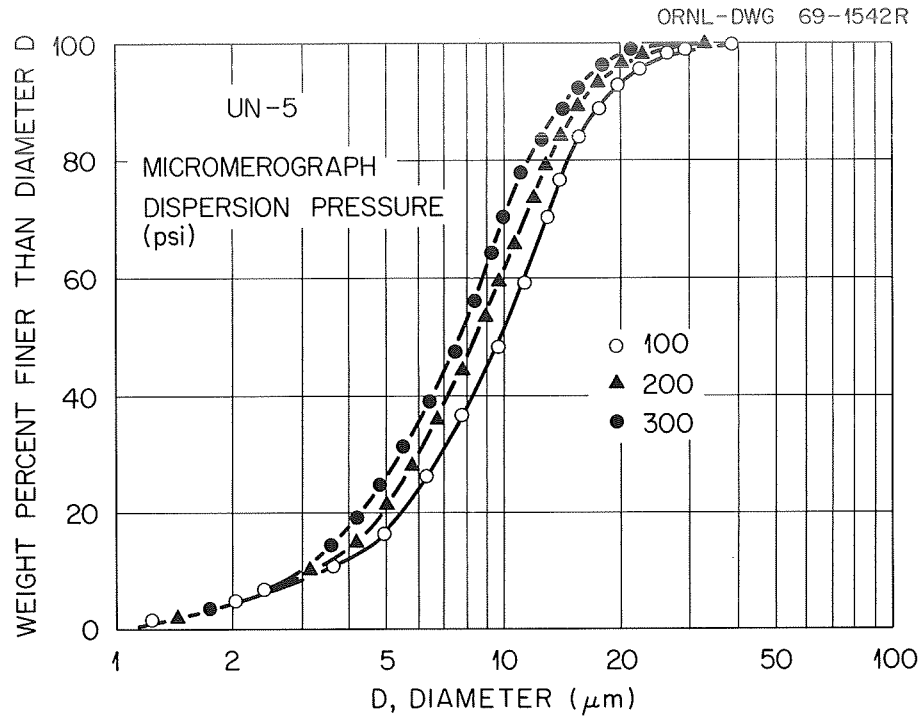


Fig. 3. Dependence of Observed Curve for Distribution of Particle Sizes in a Uranium Nitride Powder Upon Micromerograph Dispersion Pressure.

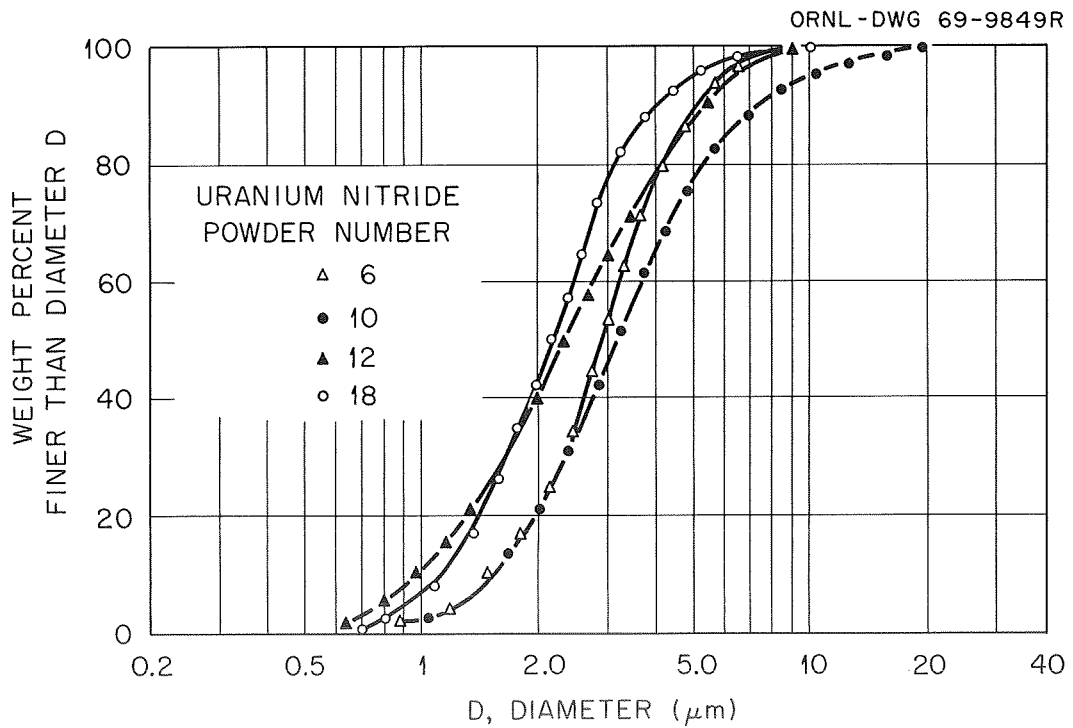


Fig. 4. Curves for Distribution of Particle Sizes Determined by Means of the Micromerograph for Several Uranium Nitride Powders.

produced in which only two of these cycles were used. The oxygen contents of the powders X-4 and X-5 were about 200 ppm O after synthesis. A comparison of the distribution curves for these powders and powder 18, for which six cycles were used, is shown in Fig. 5. Very little actual coarsening was accomplished by the experiment. In the 10-g samples,

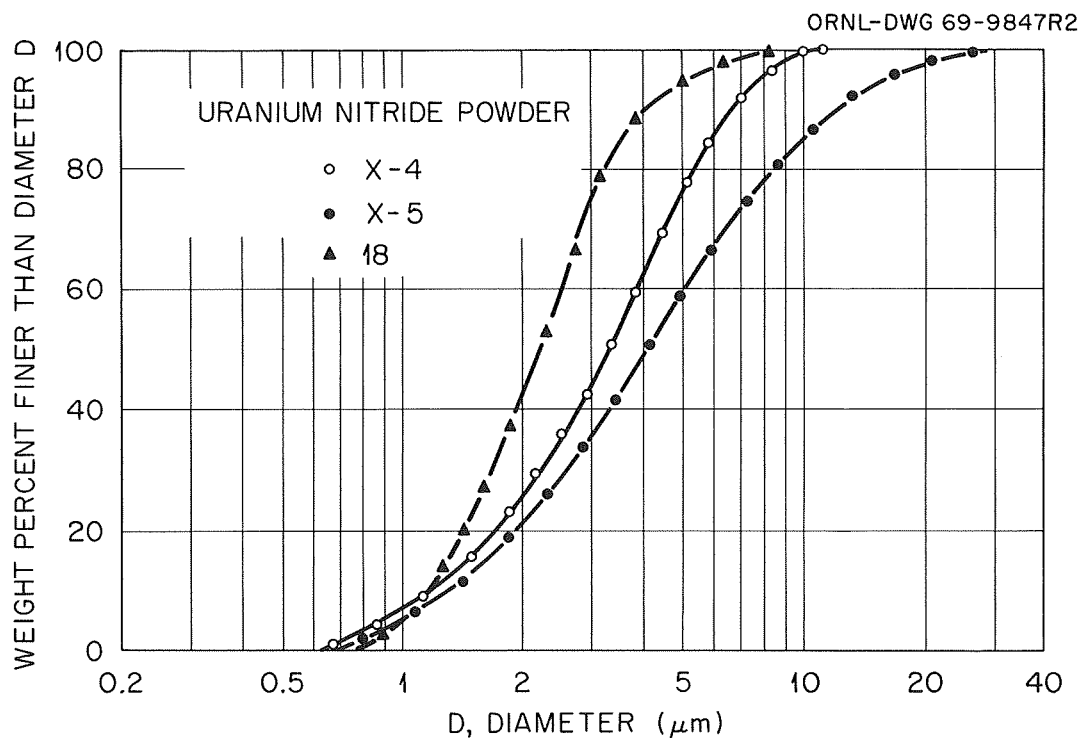


Fig. 5. Variation in the Distributions of Particle Sizes with Hydriding Treatment in Uranium Nitride Powders.

complete metal fragmentation was possible with 2 to 3 cycles. This was not the case for a 1-kg batch for which only two cycles were used. Reducing the number of hydride-dehydride cycles below six in the large-scale equipment led to some rather sizeable pieces of uranium that were not fragmented properly by the hydriding reaction. In the case of a 1-kg batch employing only two hydride cycles, a piece of metal weighing about 0.15 kg was recovered intact from the reaction chamber after completion of the nitride step. This approach to coarsening of the powders was not pursued further.

THE MORPHOLOGY OF URANIUM NITRIDE PARTICLES

The actual shape of the uranium nitride powder particles was of interest because the fabrication properties of a ceramic material are often strongly controlled by the morphology of the particles and the distribution of particle sizes. Two methods were investigated for actually studying the shapes of the particles: the electron microscope and the scanning electron microscope. Specimens of nitride particles for the electron microscope were dispersed in a parlodian film placed on a microscope grid; the features of the particle were deduced by studying the shadows of the particles in the electron beam, as shown in Fig. 6. The images observed indicated that the particles had many protrusions on their surfaces and that the objects observed in the field had dimensions of the order of those deduced from the measurements of particle size noted earlier. Considerable agglomeration is visible in Fig. 6.

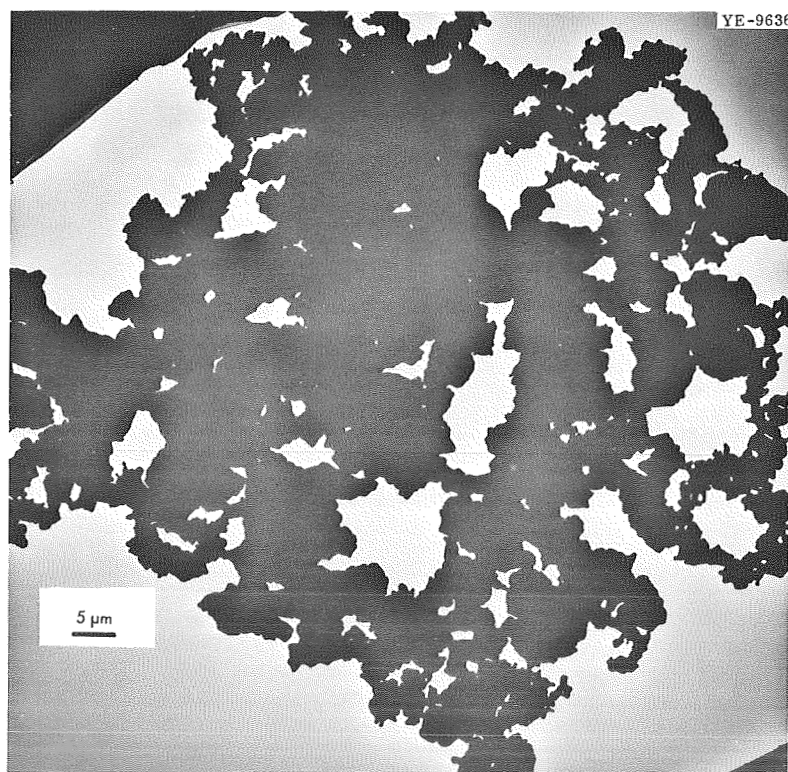


Fig. 6. Electron Photomicrograph of Uranium Nitride Particles Prepared by Twelve Hydriding Cycles.

A uranium nitride powder specimen placed gently onto a microscope grid to avoid fragmentation is shown in Fig. 7; the individual particles visible are 2 to 8 μm in extent. Spatulating the same particles with parlodian in amyl acetate produced specimens as shown in Fig. 8. The particles were dispersed and broken to some extent by the spatulating procedure. The parlodian films that surrounded the particles in the samples protected them sufficiently from oxidation during the spatulation and insertion into the microscope. The particles shown in Fig. 8 vary from 0.1 to 2 μm in extent.

We used a scanning electron microscope to examine the powder particles, since the great depth of field available with this instrument permitted the straightforward examination of entire clusters of nitride particles and required very little preparation of the specimens. The uranium nitride particles were removed from an argon-filled bottle and

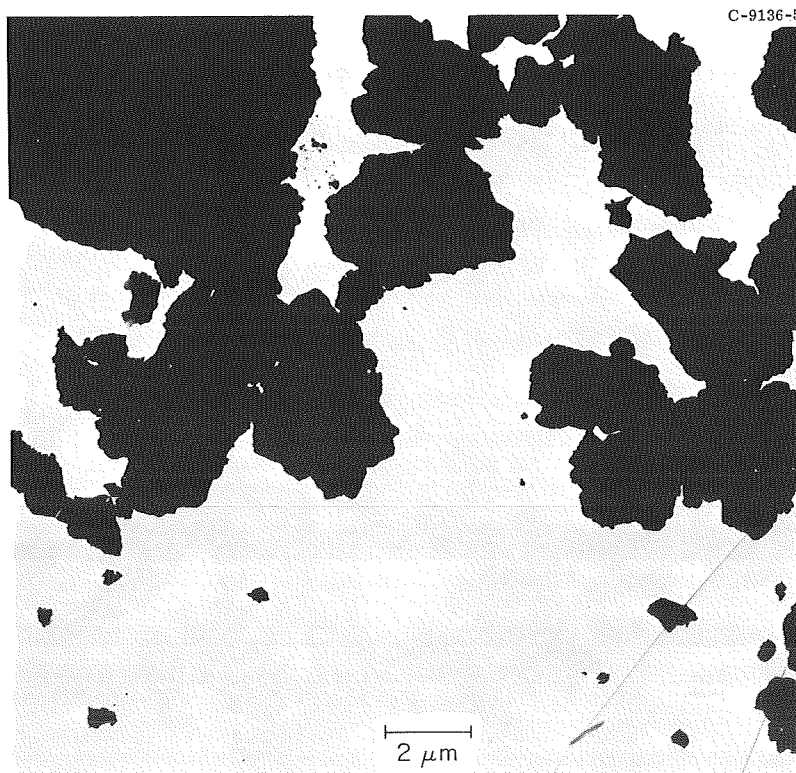


Fig. 7. Electron Photomicrograph of Uranium Nitride Particles, UN-5, Placed Gently Upon Specimen Grid.

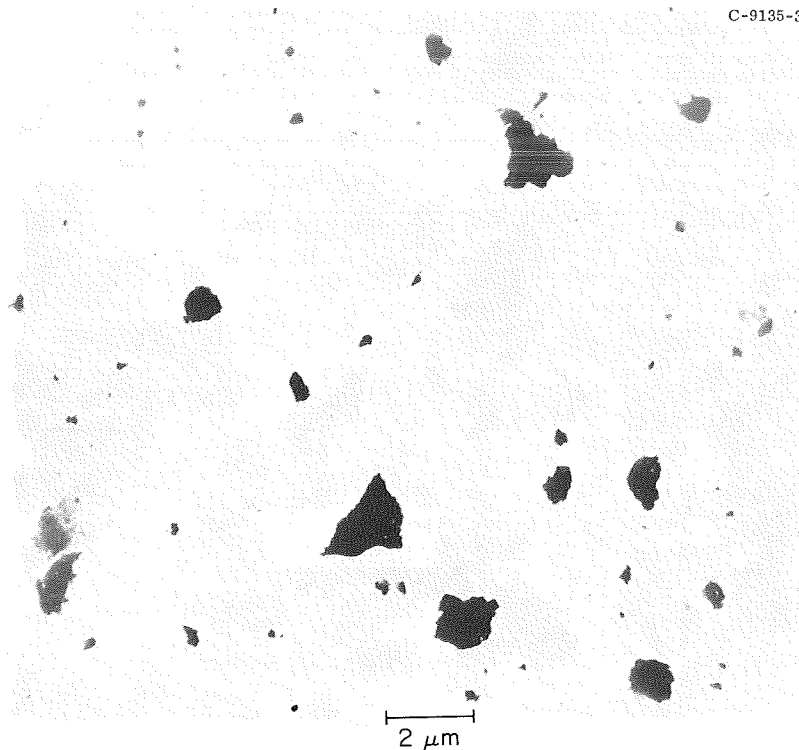


Fig. 8. Electron Photomicrograph of UN-5 Particles After Spatulation.

sprinkled onto a chilled, copper, specimen block. The block was then quickly inserted into the microscope, and the microscope column was evacuated. The powder particles had sufficient electrical conductivity and their density upon the copper block was such that no problems of charge accumulation on the specimen were encountered.

Figure 9 shows a group of particles from powder 18. Several agglomerates are visible as are the machining marks on the copper specimen block. Part of the same field is shown in Fig. 10 at a higher magnification. The particles are very irregular, and the surfaces of the particles have several bumps and protrusions on them. The observable dimensions of these particles are in good agreement with the results of the analyses of particle sizes discussed above.

Examinations with both the electron microscope and the scanning electron microscope indicated that the nitride particles were irregular in shape, had very irregular surfaces, and were essentially of the size indicated by the Micromerograph and the optical microscope.

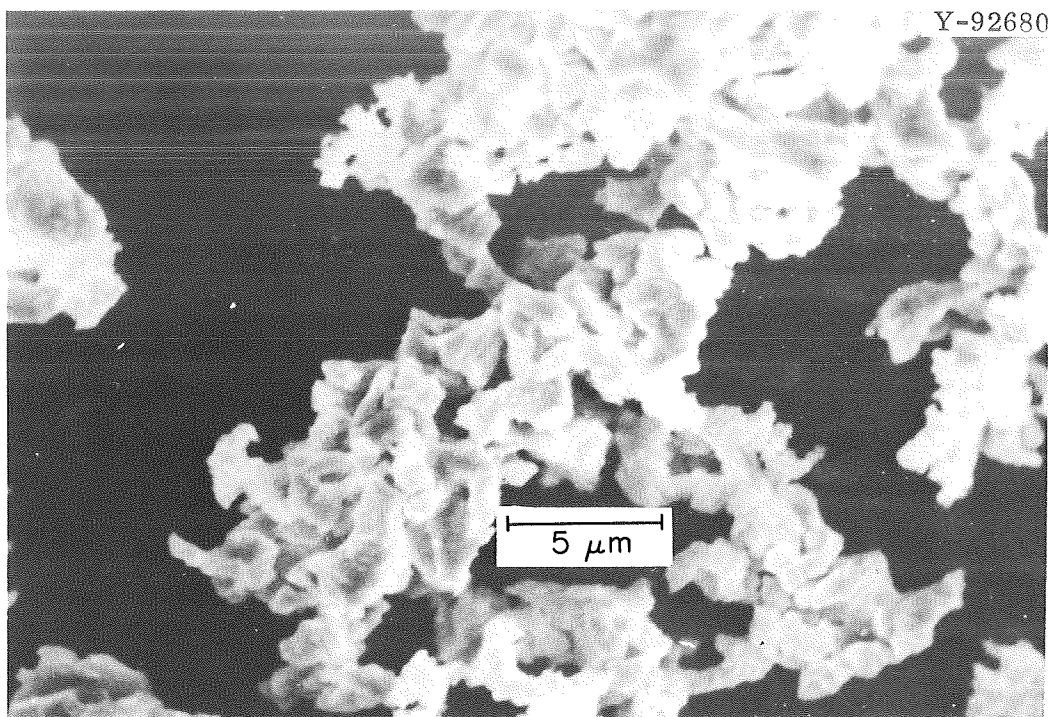


Fig. 9. Uranium Nitride Particles Placed Gently Upon Specimen Holder of Scanning Electron Microscope.

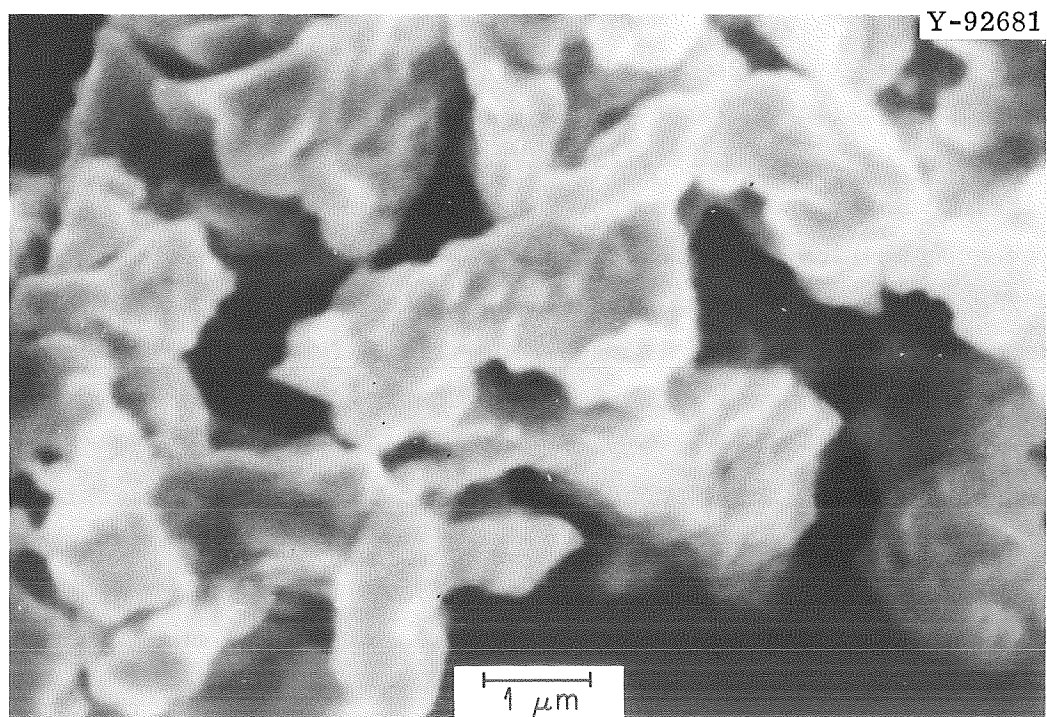


Fig. 10. Higher Magnification of Same Field as Shown in Fig. 9.

FABRICATION OF URANIUM NITRIDE

The sensitivity of fine uranium nitride powders to oxidation requires that all fabrication be done within a high-quality inert atmosphere in a glove box or that the powder be completely isolated from the oxygen in the atmosphere if part of the fabrication process takes place outside the glove box. Both uniaxial and isostatic pressing were investigated.

The morphology and hardness of the uranium nitride particles make fabrication by uniaxial pressing difficult. Since uniaxial pressing utilizes metal dies for shaping the fabricated piece, the powder particles must be able to flow within the die when the load is applied to the die punches in order to achieve a uniform fabricated or green density. If this does not occur, the piece will shrink unevenly when sintered at high temperature, and this will result in distortion, possible cracking, and a variation of the density within the piece. The many protrusions present on the surfaces of the nitride particles inhibit them from sliding by each other when the load is applied to the die. This difficulty can be reduced by lubricating the particles with an appropriate substance and lubricating the die walls with another appropriate inert substance. Very little work has been done to determine appropriate inert lubricants for uranium nitride powders. These materials must not oxidize the powder when they are mixed together nor contaminate the nitride during sintering. Camphor is one known substance that is fairly stable relative to the nitride and acts both as a lubricant to the particles and as a protector against oxidation in case the fabricated parts are exposed to an atmosphere that contains oxygen. The camphor is mixed with the nitride by first dissolving the camphor in acetone and then mixing the nitride with the camphor-acetone solution and continually blending this material while the acetone evaporates.

The process outlined above has several serious disadvantages. It is very time consuming, and the large amounts of organic vapors which have to be handled lead to serious contamination of the glove-box atmospheres and the purifiers used to maintain the quality of these atmospheres. Cracking and separation of the ends of the cylindrical parts fabricated by uniaxial pressing are common and often become evident only after the part has been machined. Sintering of the parts that contain camphor is laborious in that large volumes of this organic

must be pumped away by the furnace vacuum system. Since this results in contamination of the pump oils with camphor, the oil in the diffusion and foreline pumps must be changed frequently. We also discovered that the use of camphor leads to about four to five times more oxygen contamination of the sintered UN than that which occurs when no camphor is used in the fabrication process.

Fabrication of uranium nitride by isostatic pressing has several advantages over uniaxial pressing in that it requires no lubricant or binder mixed with the powders in some cases. The morphology of uranium nitride particles leads to very desirable characteristics in isostatically pressed parts. The particles, once forced together under large hydrostatic pressures, form a strong green part that can be handled without breakage. It has been reported by Metroka⁷ that isostatically pressed UN powder from ORNL which was sintered in a flowing argon-nitrogen mixture decreases the original oxygen and carbon content.

Several experiments in a joint effort between the Lewis Research Center of the National Aeronautics and Space Administration (NASA-Lewis) and ORNL were performed to determine whether fairly complex parts, such as annular cylinders of uranium nitride, could be fabricated by isostatic pressing. The forms used for shaping the parts were cylindrical rubber bags closed at one end. The bags were filled with nitride powder within the glove box and vibrated to increase the packing density of the powder. The top was then sealed with a rubber stopper, and the bag was evacuated. The bag was then removed from the glove box and placed in another bag filled with ethyl alcohol, and this bag was sealed. The assembly was then pressed in an isostatic press at 60,000 psi (41.4×10^7 N/m²), with water used as the hydrostatic medium. Pressure was maintained for about 2 min.

An experiment was done to establish where the fabricated piece was contaminated with oxygen and to determine if CO₂ or dry ice were adequate to protect the nitride from oxidation during transfer to the furnace facility. The results are shown schematically in Fig. 11. The oxygen analysis made after isostatic pressing indicated that the surface of the 0.4-in.-diam (1.016×10^{-2} m) rod had acquired about 770 ppm O during fabrication. The rubber bag was a latex-base rubber, and the nitride

⁷R. R. Metroka, Fabrication of Uranium Mononitride Compacts, NASA TN D-5876 (July 1970).

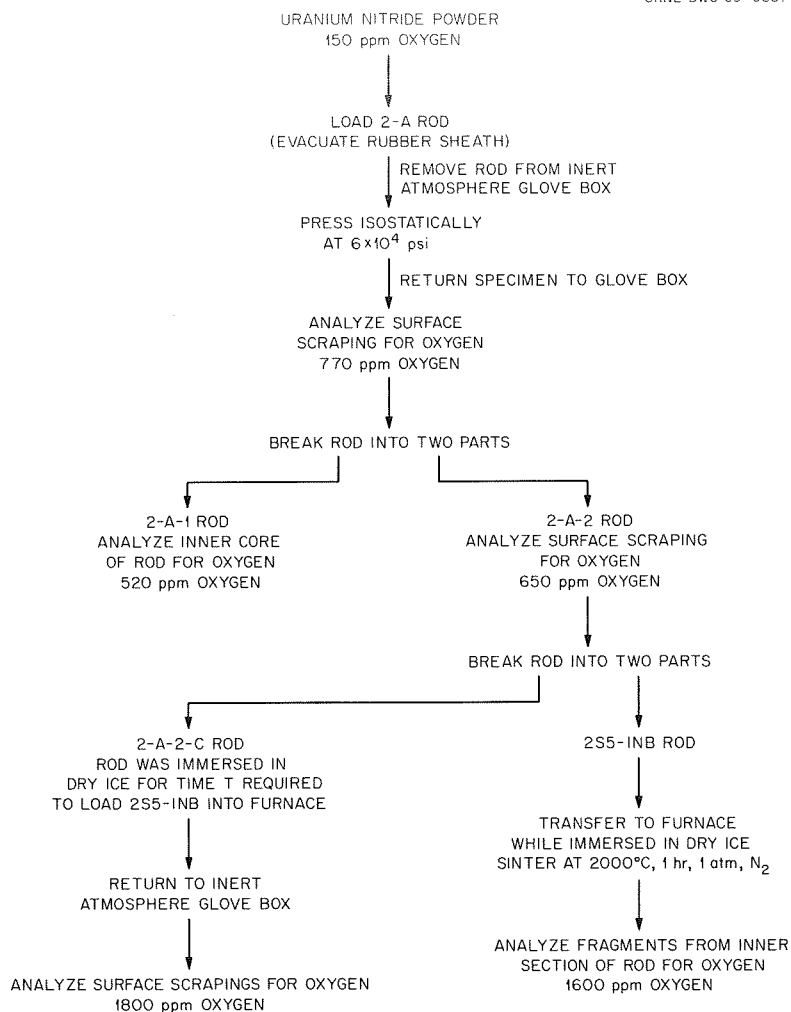


Fig. 11. Flowsheet for Experiment to Determine Oxygen Contamination of Isostatically Pressed Rod of Uranium Nitride.

apparently acquired some oxygen from this rubber, probably during the pressing operation, since a previous experiment had demonstrated that mere contact of the nitride with the rubber did not lead to the oxygen contamination noted in Fig. 11.

The inside of the rod was analyzed for oxygen and found to be contaminated less than the surface. The 2-A-2 (see Fig. 11) portion of the rod was then broken into two parts, and the 2-A-2-C portion was immersed in dry ice for the exact time necessary for the 2S5-INB portion of the specimen to be loaded into a vacuum furnace. Surface scrapings of the 2-A-2-C portion indicated that the nitride had oxidized appreciably during its contact with the dry ice; levels of about 1800 ppm O were typical. Samples taken from the interior of the sintered rod contained somewhat less oxygen (about 1600 ppm O). This work clearly indicated

that to maintain the highest possible purity in the uranium nitride before sintering, the fabricated parts must be handled only in very pure argon or other inert atmospheres.

Several long rods fabricated from the nitride powders were reasonably strong after fabrication and could be handled in the glove box and furnace loading operations.

Several large solid cylinders were then fabricated by this method to demonstrate that rods up to 0.8 in. (2.032×10^{-2} m) in sintered diameter and over 1.5 in. (3.8×10^{-2} m) long could be made. About 15 smaller rods were also fabricated with sintered lengths up to 2 in. (5.08×10^{-2} m). This sintered UN typically contained 100 to 300 ppm O. The sintering schedule for the parts involved heating them in vacuum to 1500°C (1773 K) and then to 2200 to 2300°C (2473 to 2573 K) in nitrogen at 760 torr (1.013×10^5 N/m²). The furnace was evacuated again at 1500°C (1773 K) upon cooling.

The two fabrication procedures used in this work are illustrated in Figs. 12 and 13. Sintered UN fabricated with the use of camphor typically contained 1200 ppm O. The lowest value observed in isostatically pressed sintered UN was 80 ppm O; values of 100 ppm O were common.

A relatively large annular cylinder is a potential form for a fuel element of UN. We performed experiments to determine if this shape could be fabricated of UN by means of isostatic pressing while maintaining high purity. The parts of the form used to fabricate large annular cylinders by isostatic pressing are illustrated schematically in Fig. 14. These forms were designed with the assistance of R. R. Metroka at NASA-Lewis. A photograph of disassembled and assembled form is shown in Fig. 15 along with a sintered, unmachined UN cylinder fabricated in it. The density of the sintered cylinder was 93.5% of the theoretical, and the true indicated run out of the inside diameter of such cylinders is typically ± 0.010 in.

The isostatic pressing form was loaded in the following sequence within the glove box. The inner guide rod was placed into a hole in the bottom of the pressing form, and the bottom pressing bag was slipped into the pressing form over the inner guide rod. The bottom cushion pad and washer were inserted into the bottom bag. These were necessary to

ORNL-DWG 70-3865

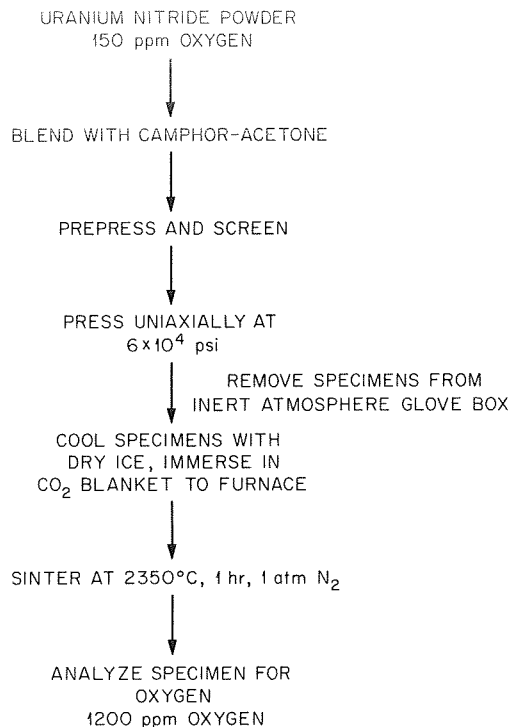


Fig. 12. Process for Fabricating and Sintering High-Purity UN.

ORNL-DWG 70-3864

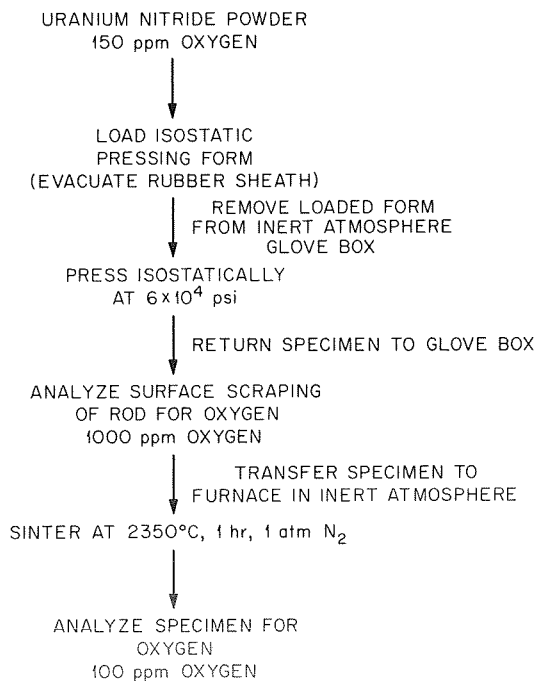


Fig. 13. Process for Fabricating UN by Uniaxial Pressing.

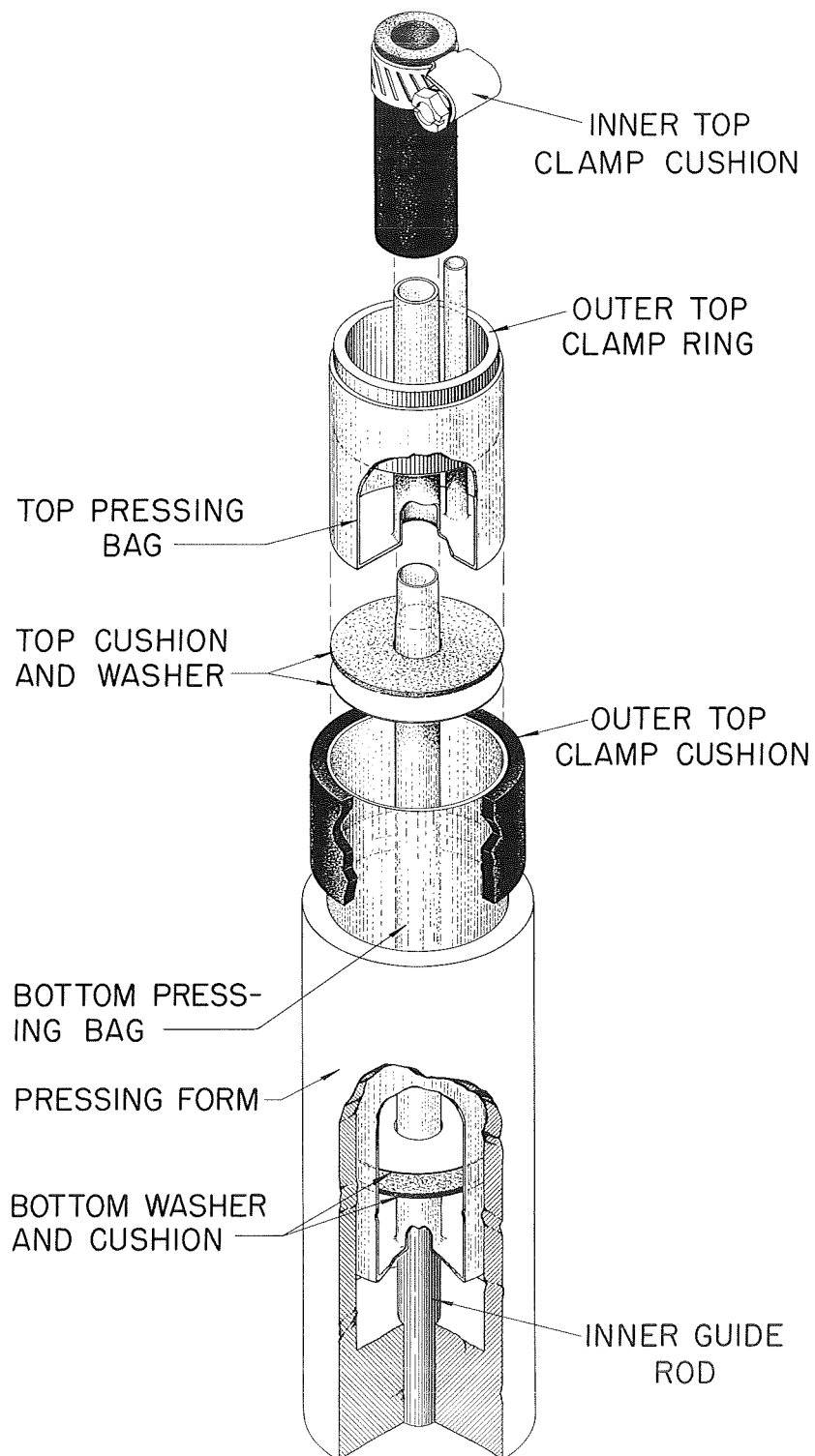


Fig. 14. Schematic Diagram of Form Used for Isostatic Pressing of UN.



Fig. 15. Mold Components for Isostatic Pressing and an Unmachined, Sintered UN Cylinder Made by This Process.

prevent the bottom bag from forming a dimple in the bottom of the piece around the inner hole during isostatic pressing. The nitride powder was loaded into the bottom bag in small quantities, perhaps one-tenth of the total loading at a time, and tamped with the powder-tamping cylinder shown in Fig. 15. The loading had to be done very carefully to maintain a reasonably constant outside diameter along the length of the final sintered piece. The inner guide rod maintained the concentricity of the bottom pressing bag during the powder filling process. When the form was completely filled with powder, the top washer and cushion were positioned on top of the loaded powder within the bottom pressing bag. The top pressing bag was then positioned in the top of the bottom pressing bag and the inner guide rod withdrawn from the inside of the bottom pressing bag, which was still within the pressing form. The inner top clamp ring was positioned in the top of the inside of the top pressing bag. The outer top clamp ring was positioned within the top of the top pressing bag, and outer and inner top clamp cushions were put in place. Hose clamps were then tightened around these cushions to provide a seal against contamination by the atmosphere and pressing fluid. The bag was evacuated with a vacuum pump through the small tube shown in the top of the top pressing bag in Figs. 14 and 15. This tube was then sealed off with a clamp.

The assembled pressing mold shown in Fig. 15 was then removed from the glove box and placed in a rubber bag that contained a fluid such as ethanol or acetone. This bag was sealed and isostatically pressed as described previously.

After pressing, the mold was removed from the containment bag and dried by placing it in the vacuum vestibule of the glove box and pumping to a pressure of 4×10^{-4} torr (5.33×10^{-2} N/m²). The vestibule was then filled with high-purity argon, and the assembled mold was transferred to the glove box and unloaded.

Several nitride cylinders were fabricated by this process, and the various fabricated and sintered dimensions and immersion densities of some of these are shown in Table 1. From the data currently available, it appears that the firing shrinkage of the nitride can be correlated with the nitrogen content of the powder when the powders are made in the same synthesis apparatus. As noted previously, the nitrogen content

Table 1. Characteristics of Large Isostatically Pressed and Sintered^a UN Cylinders

Specimen	Outside Diameter			Inside Diameter			Length			Density (% of theoretical)	Powder Designation
	Green (in.)	Sintered (in.)	Shrinkage (%)	Green (in.)	Sintered (in.)	Shrinkage (%)	Green (in.)	Sintered (in.)	Shrinkage (%)		
V-16 ^b	1.062	0.842	20.7	0.264	0.209	20.8	2.083	1.625	22.0	92.9	2S blend
V-17 ^b	1.051	0.837	20.4	0.263	0.212	19.4	2.157	1.675	22.3	93.4	2S blend
V-18 ^b	1.048	0.836	20.2	0.263	0.217	17.5	2.153	1.688	21.6	92.9	2S blend
V-19 ^b	1.049	0.839	20.0	0.266	0.216	18.8	2.161	1.700	21.3	93.4	2S blend
V-20 ^b	1.052	0.862	18.1	0.268	0.222	17.2	2.193	1.760	19.7	84.9	2S blend
B-17 ^c	0.799	0.685	14.3	0.219	0.192	12.3	1.838	1.565	14.8	92.7	3S-4
B-18 ^c	0.846	0.728	14.0	0.215	0.185	14.0	1.835	1.566	14.7	92.9	3S-4
B-20 ^c	0.858	0.738	14.0	0.217	0.185	14.8	1.862	1.580	15.1	92.9	3S-4
B-21 A ^c	0.906	0.703	22.4	0.229	0.180	21.4	2.197	1.692	23.0	93.5	2S-17
B-21 B ^c	0.898	0.699	22.2	0.229	0.180	21.4	2.098	1.620	22.8	93.7	2S-17
B-22 A ^c	0.894	0.697	22.0	0.232	0.181	21.0	2.091	1.615	22.8	93.6	2S-17
B-22 B ^c	0.894	0.716	19.9	0.232	0.186	19.5	2.009	1.602	20.2	92.9	2S-17, 3S-3 blend

^aSintering conditions for cylinders:

V-20 - 2 hr at 1800°C plus 1 hr at 1900°C.

V-16 - 2 hr at 2330°C.

V-17 to V-19 and B-17 to B-22 B - 2 hr at 2350°C.

^bFabricated with prototype pressing form similar to that shown in Fig. 14.

^cPressed with final design pressing form as shown in Fig. 14.

of the powder can vary from 5.57 to 8.11% as one varies the powder composition from $^{238}\text{U}^{14}\text{N}$ to $^{238}\text{U}_2^{14}\text{N}_3$. The 3S-4 powder used to fabricate cylinders B-17, -18, and -20 contained very little nitrogen in excess of the 5.57% in pure UN, as these cylinders lost about 0.5% by weight during the sintering process. They also had the lowest firing shrinkages, on the order of 14%. The cylinders B-21 A and B-21 B, on the other hand, lost 2.71% of their weight during on sintering, and their shrinkages were considerably higher, on the order of 22%. This difference in shrinkage cannot be accounted for because of the small difference in the final densities of the various specimens. The analyzed nitrogen content of the 2S-17 powder used in making B-21 A and B-21 B was 7.8%. The sintered cylinders weighed about 130 to 180 g.

Specimen B-22 B was a cylinder fabricated from 60% of 2S-17 and 40% of 3S-3 powder. The 3S-3 powder had a composition near UN. The addition of the 3S-3 powder reduced the shrinkages as well as the final density, as shown in Table 1.

The typical microstructure of a control specimen for V-16 is shown in Fig. 16, and the sample was single phase UN. The oxygen content of

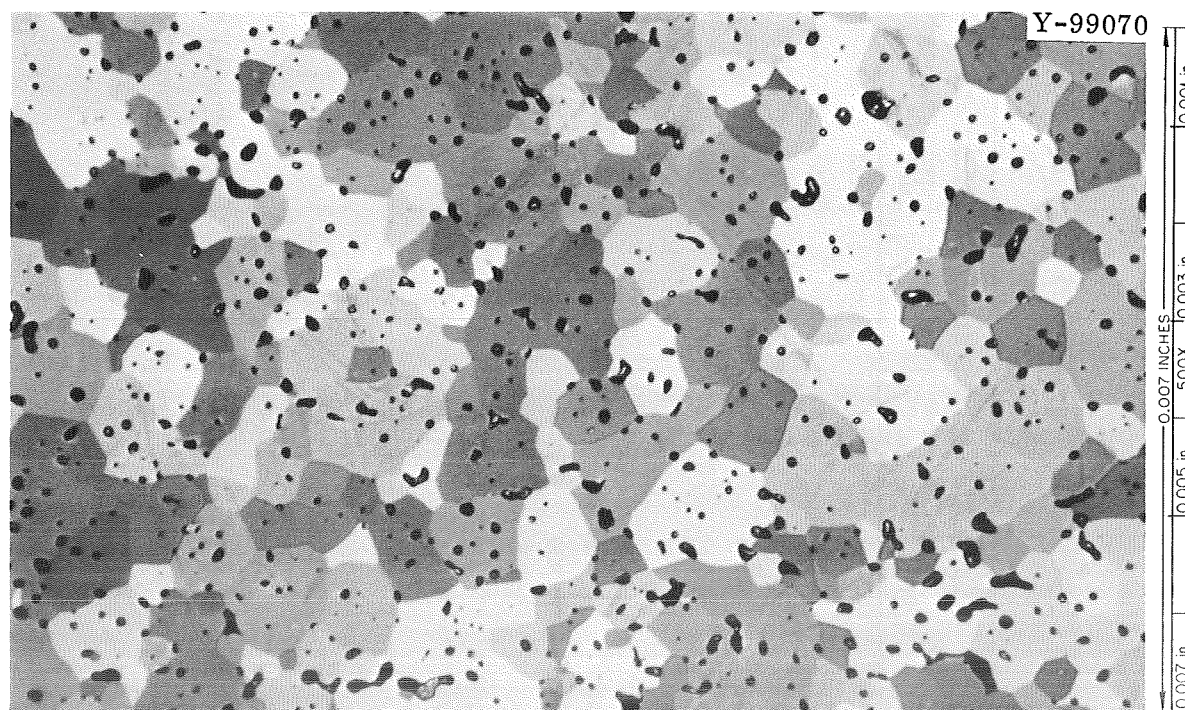


Fig. 16. Microstructure of Specimen V-16, a Large Cylinder Made by the Isostatic Pressing Process.

the UN produced in this manner is typically 100 to 300 ppm O. The oxygen content of specimen B-18, for example, was 120 ppm as determined by the inert-gas-fusion technique.

QUANTITATIVE CHEMICAL ANALYSIS OF UN

The complete characterization of a given material must include chemical analyses that will account for all of the major elements present with a certainty sufficient to permit correlations between property changes and real changes in the chemical composition. Chemical analyses of all the major elements is always a problem in nonmetallic materials, since the techniques required for one given material are usually not exactly suitable for another. A special development is then required for the analysis of each element in each material.

Considerable effort was expended to identify the analytical problems associated specifically with sintered UN, since the problems associated with the analysis of mixtures of UN and U_2N_3 or U_2N_3 alone are somewhat different. Many analyses were performed at ORNL and at other laboratories where there was previous experience in analyzing sintered pellets of UN.

The analysis of small UN specimens for uranium, nitrogen, oxygen, and carbon with high precision was the first practical objective. The first problem was to define "high precision." Analyses, to be really useful, should have sufficient precision to provide meaningful information about the absolute accuracy and thereby the actual composition of a specimen within close limits. This condition requires that the precision of the analyses for uranium and nitrogen be considerably better than those for oxygen and carbon, because the latter two elements are present in relatively small concentrations.

A Comparative Chemical Analysis Experiment or "round robin" was initiated, with four analytical laboratories participating, to evaluate the nature of any existent problems. The analyses were performed at ORNL, Battelle Memorial Institute, LeDoux and Company, and NASA-Lewis. The specimens consisted of two sets of pellets, weighing about 4 g each, designated R452 and R459. The specimens R452 were prepared so as to have an oxygen content that led to the presence of an oxide

phase within the microstructure, and those of R459 were prepared so as to exhibit only the typical equiaxed structure of very dense UN.

The specimens of a given set were fabricated from the same powder at the same time and were sintered together at 2300°C (2573 K) for 4 hr at 760 torr (1.01×10^5 N/m²) of nitrogen. The specimens were positioned on a setting plate of tungsten as illustrated schematically in Fig. 17.

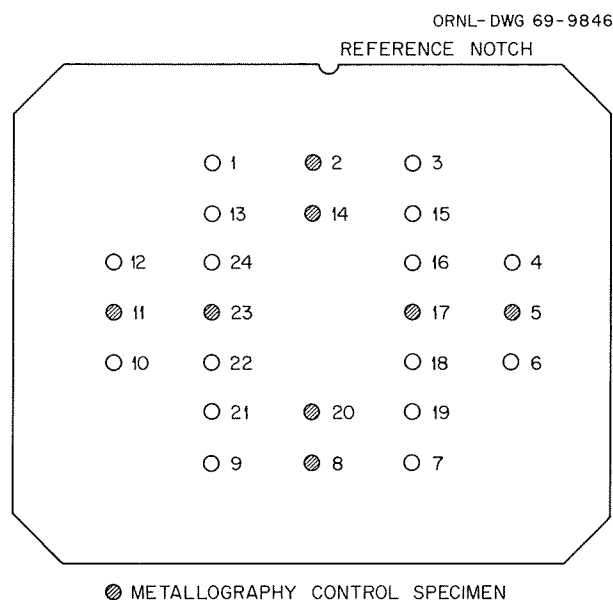


Fig. 17. Schematic Diagram of Specimen Locations for Sintering on the Tungsten Setting Plate in Comparative Chemical Analysis Experiment.

The plate was about 1.97 in. (5×10^{-2} m) on a side. The numbers designate the individual pellet specimens (thus, R459-18, for example, represents specimen 18 from set R459) so that we would be able to look for correlations between the chemical results and position on the setting plate. Representative microstructures of R452 and R459 are shown in Fig. 18(a) and (b), respectively.

Each site received four specimens from a given set. The microstructure of each microscopy control specimen was examined thoroughly at 250 and 500X, and all of the microstructures of the samples indicated by cross-hatching in Fig. 17 were identical within a given set and looked like those shown in Fig. 18. To ensure that the samples were not inadvertently contaminated during shipment, each pellet was sealed in

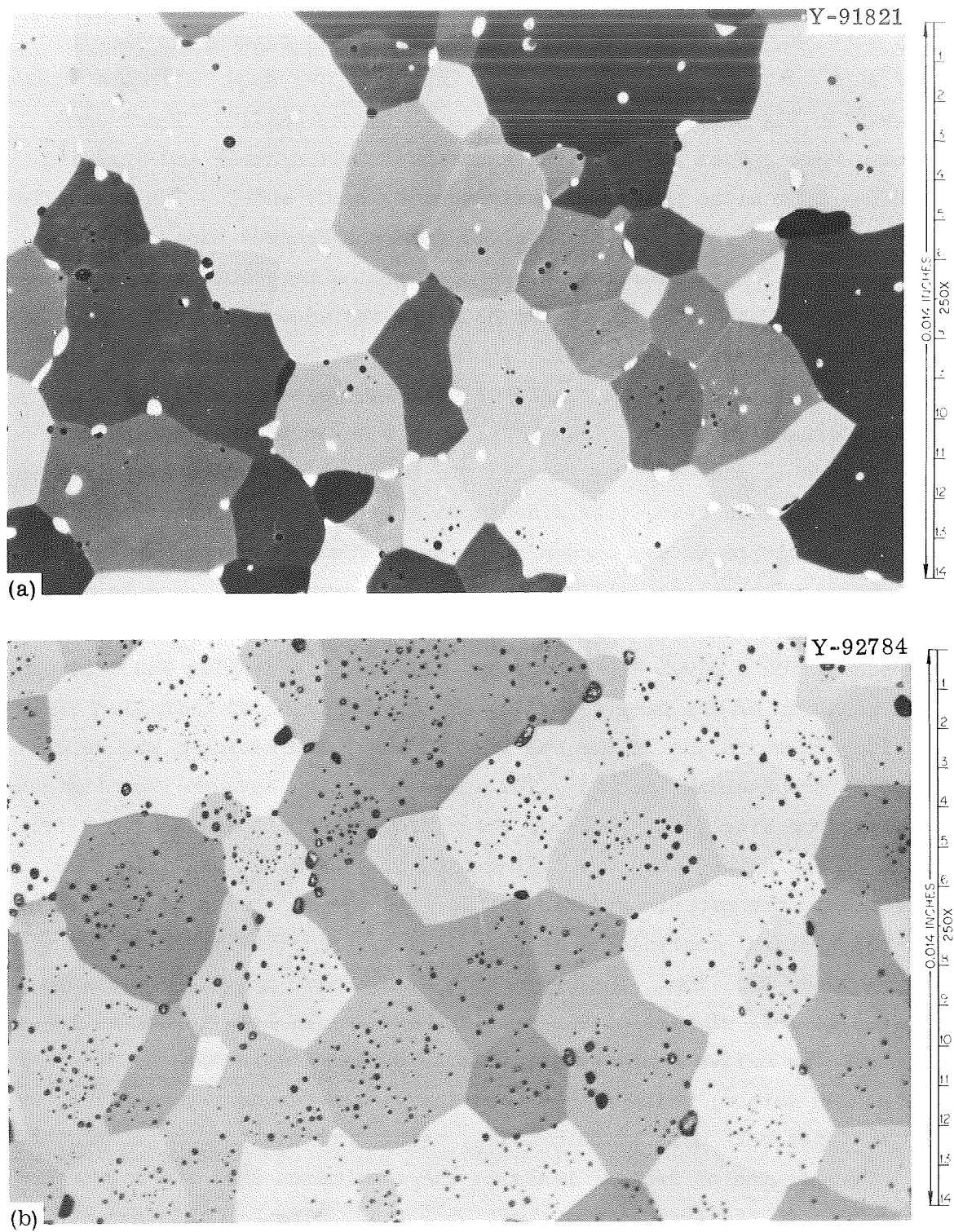


Fig. 18. Microstructure of Specimens (a) R452-14 and (b) R459-5.

very pure argon within a capsule, like that shown cutaway in Fig. 19. Four such capsules were placed in a steel transfer tube, like that shown cutaway in Fig. 20, and welded shut in very pure helium. These containers were opened at the sites under inert atmospheres and analyzed.

The four sites have been designated A, B, C, and D. The identification of these sites may be obtained from the Project Manager at NASA-Lewis. The results for the R452 specimens were obtained first and are given in Table 2. All of the data are included, and each number represents a specific analysis. In the case of R452, site A had only enough sample to perform a single uranium analysis per specimen plus all the others required. Site D was unable to do the oxygen analyses for samples 22 and 24. The results for the R459 specimens are given in Table 3. In this case, site C could do only a single uranium analysis and was unable to do any oxygen analyses on the specimens. It should be emphasized here that all of the sites had prior experience in analyzing sintered UN. All of the sites used basically the same analytical techniques for a given element except oxygen. The uranium was determined by combustion of the sample to U_3O_8 and gravimetric determination of the uranium concentration in the starting sample. The nitrogen was determined by the Kjeldahl method. The major deviation between the nitrogen results from site C for R452 and those from other sites has been attributed to the method used for dissolving the sample and oxidizing the nitrogen to the proper oxidation state. In the digestion process required for the Kjeldahl analysis it is necessary to transform the nitrogen in the UN to an NH_4^+ ion. The production of nitrogen gas can occur with subsequent loss of part of the sample, which would lead to low nitrogen values. The oxygen analyses of sites A, B, and D were done by the inert-gas-fusion method, while site C used the vacuum-fusion method. The carbon analyses were done by combustion, using chromatographic techniques.

Examination of Table 2 leads to the conclusion that the oxygen concentration in the samples was about 3500 ppm. Site D had inadequate sample handling methods at the time of this analysis to avoid oxygen contamination, and the data from site C do not permit a rational conclusion to be made. A point count with an optical microscope of the oxide phase of all of the metallography control samples for R452

Photo 94207



Fig. 19. Individual Pellet Capsule for Comparative Chemical Analysis Specimen.

Photo 94206

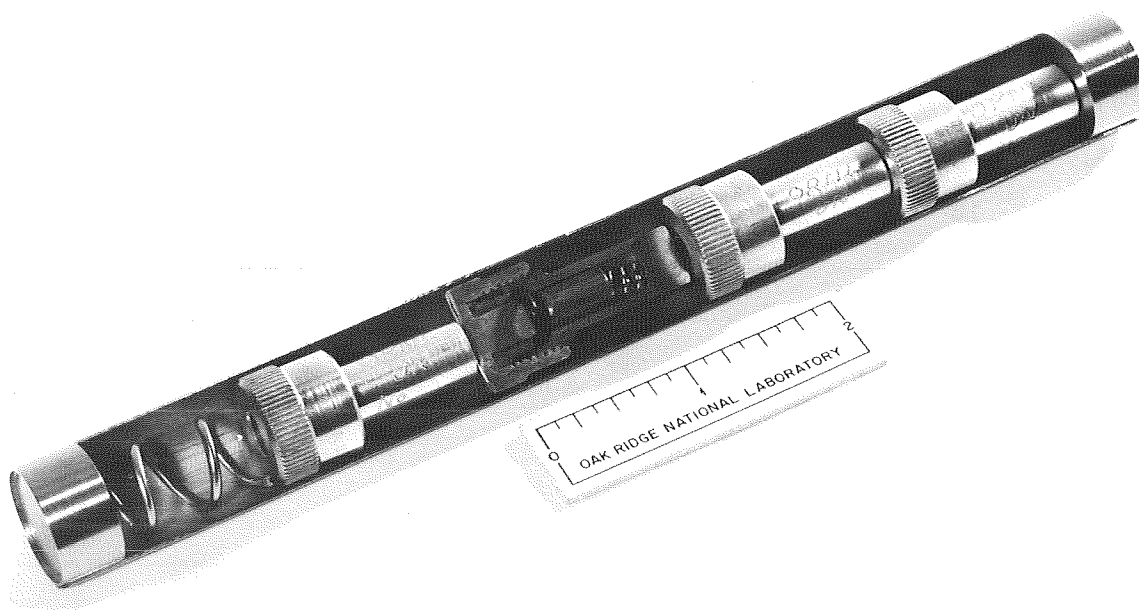


Fig. 20. Shipping Tube for UN Chemical Analysis Samples for a Given Site.

Table 2. Comparative Chemical Analyses for Uranium Nitride
Sintering Run R452

Sample	Composition, %			
	U	N	O	C
<u>Site A</u>				
1	94.37	5.22	0.35	0.052
		5.15	0.35	0.054
3	94.41	5.19	0.34	0.051
		5.18	0.35	0.051
13	94.36	5.14	0.38	0.053
		5.14	0.36	0.055
15	94.35	5.20	0.34	0.051
		5.24	0.36	0.053
<u>Site B</u>				
7	94.28	5.27	0.37	0.057
	94.31	5.24	0.37	0.058
9	94.26	5.27	0.38	0.063
	94.22	5.29	0.37	0.064
19	94.31	5.22	0.38	0.057
	94.34	5.25	0.37	0.057
21	94.26	5.26	0.37	0.066
	94.18	5.30	0.37	0.065
<u>Site C</u>				
4	94.75	4.80	0.40	0.059
	94.58	4.83	0.44	0.061
6	94.59	4.79	0.29	0.062
	94.55	4.85	0.29	0.057
16	94.66	4.79	0.28	0.055
	94.62	4.83	0.29	0.054
18	94.64	4.83	0.27	0.058
	94.58	4.83	0.27	0.061
<u>Site D</u>				
10	94.40	5.23	0.47	0.066
	94.32	5.19	0.45	0.066
		5.23		
12	94.27	5.19	0.46	0.066
	94.11	5.14	0.47	0.066
		5.31		
22	94.12	5.24		0.063
	94.13	5.26		0.063
		5.20		
24	94.01	5.22		0.062
	93.90	5.20		0.066
		5.22		

Table 3. Comparative Chemical Analyses for Uranium Nitride
Sintering Run R459

Sample	Composition, %			
	U	N	O	C
<u>Site A</u>				
10	94.70	5.12	0.21	0.020
	94.66	5.10	0.20	0.020
12	94.52	5.27	0.20	0.023
	94.74	5.13	0.20	0.025
22	94.63	5.11	0.21	0.019
	94.62	5.19	0.21	0.018
24	94.66	5.18	0.21	0.021
	94.56	5.19	0.21	0.018
<u>Site B</u>				
4	94.28	5.34	0.21	0.017
	94.22	5.35	0.20	0.019
6	94.29	5.40	0.20	0.019
	94.24	5.26	0.20	0.019
16	94.28	5.25	0.22	0.025
	94.28	5.29	0.22	0.027
18	94.38	5.34	0.22	0.027
	94.30	5.37	0.23	0.028
<u>Site C</u>				
7	94.51	5.30		0.10
		5.26		
9	94.53	5.29		0.11
		5.33		
19	94.50	5.20		0.11
		5.13		
21	94.51	5.21		0.11
		5.30		
<u>Site D</u>				
1	94.56	5.20	0.24	0.048
	94.56	5.23	0.23	0.049
			0.23	
3	94.47	5.35	0.23	0.043
	94.54	5.28	0.23	0.048
			0.25	
13	94.52	5.32	0.27	0.046
	94.53	5.27	0.26	0.052
			0.26	
15	94.62	5.27	0.22	0.036
	94.51	5.29	0.22	0.038
			5.26	

resulted in a total of 48,019 counts. The oxide counts indicated an average concentration of $1.92 \pm 0.04\%$ (volume) of UO_2 based on the assumption that the oxide phase was $\text{UO}_{2.000}$; this concentration corresponds to $1.48 \pm 0.03\%$ (weight) of UO_2 or 1746 ± 39 ppm O. The method used for polishing the UN was found to be critically important for point counting. Specimen R452-2 was hand polished and yielded a point count of 82/6082 or $1.38 \pm 0.13\%$ UO_2 , whereas the same specimen after Syntron polishing yielded 98/5718 or $1.71 \pm 0.12\%$ UO_2 by volume. If one assumes that approximately 1750 ppm O was present in the nitride as $\text{UO}_{2.000}$, then about 1800 ppm O was present in solid solution in the mononitride itself.

Analysis of the data for R459 is, in principle, easier, since no second-phase oxide was visible in these specimens. First, it is fairly obvious from Table 3 that these specimens contained about 2300 ppm O and less carbon than did R452. No oxide phase was detected in any of the microscopy samples even when they were examined at 1000X. This oxygen content was higher than the 1800 ppm deduced to be in solid solution in the R452 specimens in the presence of second-phase oxide, possibly because the second phase present in Fig. 18(a) was not $\text{UO}_{2.000}$ but an oxynitride with a crystal structure very similar to that of UO_2 . Since U_2N_3 has a structure very much like that of UO_2 , this is not unreasonable. Such a situation would lead to a higher actual oxygen concentration in the UN grains of R452 than the 1800 ppm mentioned previously. The maximum solubility of oxygen in the UN for the given thermal history could not be established from the available data. Previous work by Godfrey⁸ indicated that the oxide phase precipitates in UN first as sub-microscopic particulates before it becomes visible as a discrete phase, as shown in Fig. 18(a). Our work did not provide enough data to establish the exact mechanism or the condition for the phase separation.

Table 3 indicates that there are problems that prevent the accurate quantitative analysis of UN at the present. For example, if we arbitrarily choose the top row of results for R459-10 analyzed at site A, the mass balance is 100.05%, whereas for R459-4 analyzed at site B the

⁸T. G. Godfrey, Oak Ridge National Laboratory, private communication.

mass balance is 99.847%. These mass balances agree reasonably well for normal analytical procedures. However, R459-10 reportedly contained only 5.12% N and only 5.34% nonmetallic atoms, while 5.556% is the theoretical value for $^{238}\text{U}^{14}\text{N}$. The nonmetal balance for R459-4 is 5.567%, or slightly more than the theoretical limit, with 5.34% N. This type of result is typical for the data of Tables 2 and 3. A given site can have good internal consistency in its results and yet disagree markedly with another laboratory that also had reasonable internal consistency in its results. Since the specimens analyzed by sites A, B, C, and D were positioned about 0.5 to 3 cm (0.5 to 3×10^{-2} m) apart during sintering at 2300°C (2573 K), it seems unlikely that a really significant difference in stoichiometry could exist among the pellets of a given set.

After the completion of the work on the Comparative Chemical Analysis Experiment another group of sintered UN specimens was quantitatively analyzed for the major and minor elements, (i.e., uranium, nitrogen, carbon, and oxygen). The microstructures of samples that had identical histories were examined, and this information was used to judge the credence of the chemical results as a whole. This experiment was similar to the Comparative Chemical Analysis Experiment except that all of the analyses were done at ORNL. Each individual analysis was followed very carefully in an effort to elucidate the specific analytical problems associated with UN. The data obtained are given in Table 4. An item number designates UN of the particular ^{235}U enrichment shown, and a run number (R_--) designates a particular sintering run in which a group of pellets were densified. All of the pellets were sintered at 2300°C (2573 K) for 4 hr in a nitrogen atmosphere. These pellets were fabricated by uniaxial pressing, and camphor was used as a lubricant-binder. All of the pellets of a particular group number were made from the same nitride powder, but the pellets of a particular R number were fabricated at different times. The analyses given for a specific run number were all obtained on one specific pellet. The size of the samples was such that only one uranium analysis could be made and still provide enough material for the other analyses. In the case of R467 and R480, another pellet of each was analyzed for uranium; the results

Table 4. Results of Chemical Analysis for Sintered UN Specimens

Group Number	Run Number	Enrichment (% ^{235}U)	Composition, wt %			
			U	N	O	C
1	470	10	94.76	5.40	0.165	0.024
				5.29	0.161	0.023
				5.32	0.180	
	471		94.64	5.48	0.187	0.024
				5.43	0.179	0.022
				5.13	0.190	
	482		94.67	5.29	0.180	0.023
				5.20	0.177	0.026
				5.24	0.169	
2	491	5.6	94.47	5.38	0.150	0.029
				5.33	0.149	0.022
				5.22	0.152	
	492		94.58	5.53	0.128	0.023
				5.47	0.120	0.021
				5.19	0.128	
	493		94.61	5.39	0.116	0.032
				5.33	0.114	0.024
					0.110	
	494		94.49	5.35	0.102	0.026
				5.33	0.098	0.030
				5.30	0.101	
3	467	Depleted	94.85	5.24	0.156	0.033
				5.26	0.158	0.032
				5.29	0.165	
	480		94.56	5.20	0.137	0.026
				5.22	0.141	0.028
				5.30	0.174	
4	484	Depleted	94.44	5.41	0.163	0.046
				5.33	0.140	0.046
				5.22	0.136	
	485		94.48	5.29	0.154	0.039
				5.41	0.147	0.040
				5.14	0.158	

agreed, within 0.02%, with the values given for uranium for these runs listed in Table 4.

If the results for nitrogen, oxygen, and carbon are averaged individually and transformed to molar concentrations, these values can be used as parameters for evaluating the stoichiometry of a specimen having a particular R number.

The mass balance obtained for R470, when all analyses were used to compute the averages, was 100.331%, while that for R471, excluding the 5.13% N value, was 100.041%. The mass balance for R470 was too high to be acceptable, and that for R471 was marginal, since this mass balance should include all elements present except trace-element impurities, which are known in this case to be 0.05% or less. The ratio of metals to nonmetals (M:NM) for R470 was 1.0114; thus, the ratio of nonmetals to metals (NM:M) was 0.9887, perhaps implying that the UN specimen was slightly deficient in nonmetals. The work of Benz and Bowman⁹ implied that this situation might be possible in this system at high temperatures, but it has not been demonstrated that this situation can be "frozen in" during cooling of UN from high temperatures to room temperature. The M:NM ratio of R471 was 0.9848 and the NM:M ratio was 1.0154. This implies that sample R471 was hyperstoichiometric in nitrogen or that some sesquinitride phase was retained in the sintered sample. The microstructures of specimens R470 and R471, shown in Fig. 21, appeared to be identical at both 500 and 1000X.

The results obtained indicate that two of the major problems that prevent really acceptable precision and accuracy in the analyses are associated with the analyses for uranium and nitrogen. Since these are the major elements, demonstrable precision of at least 1 part in 1000 is required, and 1 part in 5000 or 10,000 would be preferable. The accuracy, of course, must be nearly this good. The gravimetric procedures now used to analyze for uranium and the Kjeldahl method used for nitrogen simply are not precise or accurate enough to provide meaningful values for this application.

⁹R. Benz and M. G. Bowman, J. Am. Chem. Soc. 88(2), 264-268 (1966).

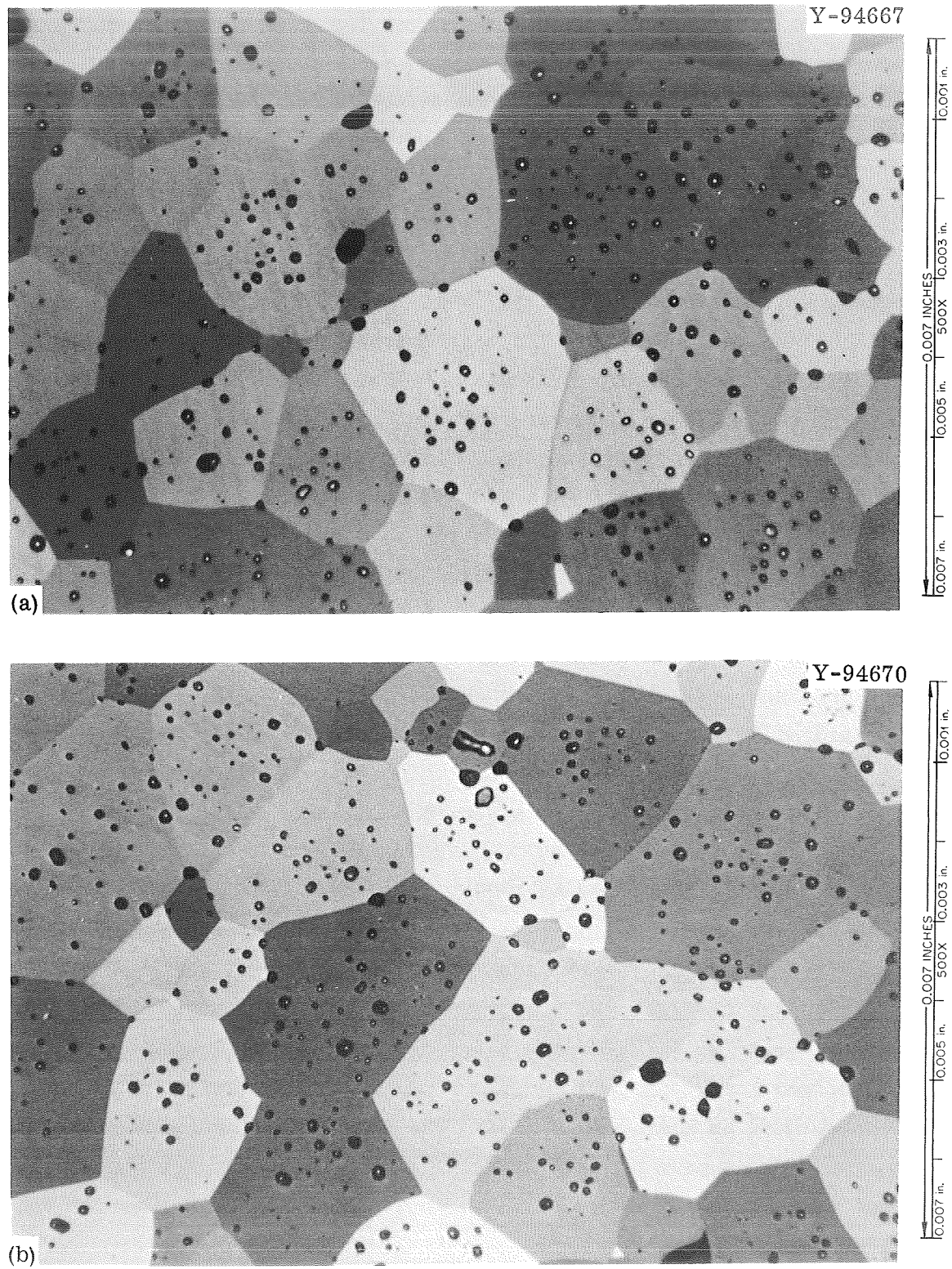


Fig. 21. Microstructures of UN Specimens (a) R470 and (b) R471.

The oxygen sampling and analysis procedures established at ORNL consistently provide fairly low scatter within a triplicate sample group, as shown in Table 4. The maintenance of the precision to levels as low as about 100 ppm O has been verified in many isostatically pressed and sintered specimens. The carbon analyses have consistently shown an acceptable scatter at levels of 200 to 300 ppm C.

Electronic methods for determining the uranium concentration in sintered specimens of UN were investigated; the results were compared with those obtained on the same pellet by use of the gravimetric combustion method. Coulometric determinations of uranium were made on both the U_3O_8 product of the gravimetric method and on aliquots of a given UN pellet that were dissolved directly and then titrated. A total of 18 specimens were investigated, and the results are given in Table 5. The samples were dense, sintered pellets of UN. They were made from various powder batches and were all sintered under the conditions noted previously, but each was sintered in a different sintering run. The enrichments in ^{235}U varied from essentially 0 to 10%. This variation changed the theoretical uranium content from 94.444% U in $^{238}\text{U}^{14}\text{N}$ to 94.438%. It also changed the theoretical nitrogen content from 5.556% in $^{238}\text{U}^{14}\text{N}$ to 5.550% in the enriched UN. These variations are obviously much smaller than the variations obtained for the uranium analyses listed in Table 5.

The analytical methods used to determine uranium content are discussed below.

1. Gravimetric Combustion of UN Sample. A sample, as chunks from a sintered pellet of UN weighing about 0.4 g, was placed in a weighed platinum boat. The boat and powder were weighed together, and the actual weight of the UN was determined as the difference. The boat and sample were placed in a muffle furnace at 400°C (673 K). The temperature of the furnace was then slowly increased to 850°C (1123 K). The sample was ignited at this temperature overnight. The boat and sample were removed from the furnace and cooled in a desiccator, and the weight of the resulting U_3O_8 was determined. The percentage of uranium was calculated from this weight.

Table 5. Comparison of Various Analytical Procedures for Determining Uranium Content of Sintered UN

Sample	Uranium Content, %		Coulometric Determination of UN
	Gravimetric Combustion	Coulometric ^a Determination of U ₃ O ₈	
1	94.76	84.73	94.70
	94.73	84.71	94.72
2	94.74	84.66	94.73
	94.80	84.63	94.69
3	94.65	84.84	94.48
	94.62	84.86	94.45
4	94.72	84.61	94.71
	94.76	84.65	94.68
5	94.45	84.76	94.41
	94.48	84.70	94.42
6	94.41	b	94.82
	94.45	b	94.87
7	94.66	b	94.76
	94.66	b	94.67
8	94.59	b	94.72
	94.55	b	94.77
9	94.39	84.86	94.40
	94.39	84.93	94.41
10	94.45	84.83	94.71
	94.45	84.62	94.61
11	94.44	84.91	94.48
	94.43	84.92	94.56
12	94.42	84.82	94.74
	94.45	84.77	94.64
13	94.35	84.70	94.40
	94.38	84.78	94.38
14	94.41	84.75	94.60
	94.44	84.70	94.50
15	94.46	84.69	94.45
	94.46	84.73	94.50
16	94.60	84.66	94.38
	94.53	84.35	94.37

Table 5. Continued

Sample	Uranium Content, %		Coulometric Determination of UN
	Gravimetric Combustion	Coulometric ^a Determination of U ₃ O ₈	
17	94.48	84.87	94.70
	94.51	84.88	94.74
18	94.50	84.80	94.53
	94.56	84.79	94.52

^aThe uranium content of $^{238}\text{U}_3^{16}\text{O}_8 = 84.80\%$; 10% enrichment in ^{235}U decreases uranium content to 84.63%.

^bThese samples were lost due to instrumental problems.

2. Coulometric Determination of the Uranium in the U₃O₈ Residue from Analysis in A. The U₃O₈ that resulted from the gravimetric combustion of UN was dissolved in HNO₃ in a 150-ml beaker. We added 10 ml of concentrated H₂SO₄ to this solution and evaporated the solution to dryness. The breaker was cooled, and the sides of the beaker were washed with distilled water. The solution was again evaporated to dryness to eliminate all traces of nitrate from the solution. The residue was then cooled and diluted to 50 ml with 5% H₂SO₄. One-milliliter aliquots of this solution were then titrated by a standard coulometric procedure for uranium.

3. Coulometric Determination of the Uranium Content of Original UN Sample. The sintered UN pellet was broken into chunks small enough that four to five of them would comprise each analytical sample. Approximately 400 mg (4×10^{-4} kg) of the broken pellet was accurately weighed and placed in a 150-ml beaker to which 20 ml of a 1:1 solution of HNO₃ and water was added. The solution was covered with a watch glass and digested with mild heating until solution was complete. We added 10 ml of concentrated H₂SO₄ to this solution and eliminated the HNO₃ by evaporation. When the dried residue was cooled and diluted to 50 ml with 5% H₂SO₄, the uranium content was determined coulometrically as described above.

Table 5 demonstrates that it is not obvious which of the three methods gives more satisfying results. The results for samples 5 and 15 agree quite closely with the theoretical value for uranium in UN. Note that 84.80% is the theoretical value expected in U_3O_8 when all of the uranium is ^{238}U in the original UN sample. For sample 3, the two coulometric methods agree quite well with the theoretical value, whereas the gravimetric method gave results that are about 0.2% above the theoretical value. The apparent scatter present in the results in Table 5 is about 1 part in 200 when either the results obtained on a specific sample or the results from different samples are compared. This is about the same variation noted for the uranium values in Table 4. The results in Table 3 for the uranium content of R459 exhibit a somewhat smaller spread if the results from site B are ignored, since this laboratory obtained significantly lower results than the other sites for the uranium analysis of this set of specimens.

The nitrogen values in Table 4 exhibit scatter as large as 0.35% for a given specimen, or about 1 part in 16. The values for specimen R494, however, had a variation of about 1 part in 100. The causes for these fluctuations have not been determined. Some of the nitrogen results in Table 3 for the R459 specimens (such as 15) exhibit much better precision while results for others (such as 6) do not. Careful analytical experiments in which several nitrogen samples are extracted from a densely sintered rod of UN would help to clarify whether the observed variations in uranium and nitrogen content are real or are due to presently uncontrolled variations in the analytical technique, since it is unlikely that an appreciable compositional variation would occur in a given sintered rod of UN at temperatures above 2000°C (2273 K).

SINTERING OF UN

The densification of fabricated cylinders of uranium nitride was determined as a function of temperature at a fixed time of 1 hr at the maximum temperature. One of the primary objectives of this effort was to establish the conditions required to produce UN with a bulk density of about 85% of the theoretical. The specimens were sintered in a cold-wall furnace that had a tungsten-mesh heating element and tungsten shields.

The specimens were fabricated by isostatic pressing with no binder, uniaxial pressing with no binder, and uniaxial pressing with a camphor binder. The specimens pressed isostatically were compacted at 50,000 psi ($34.5 \times 10^7 \text{ N/m}^2$); the specimens pressed uniaxially with camphor were pressed at 20,000 psi ($13.8 \times 10^7 \text{ N/m}^2$); the specimens pressed uniaxially with no binder were pressed at 8000 psi ($5.52 \times 10^7 \text{ N/m}^2$). Higher pressures applied uniaxially to the pure powder caused severe die seizure. The specimens were cylinders about 6 mm in diameter by 6 mm high.

The program of time, temperature, and nitrogen pressure used in sintering the specimens consisted of heating them under vacuum to 1500°C (1773 K), increasing the nitrogen pressure to 760 torr ($1.01 \times 10^5 \text{ N/m}^2$), and then increasing the temperature in a few minutes to the sintering temperature of interest. After 1 hr, the temperature was reduced to 1500°C (1773 K), and the furnace chamber was evacuated and then cooled quickly to room temperature.

The results obtained for temperatures from 1650 to 2200°C (1923 to 2473 K) are shown in Fig. 22. The densities were measured by the

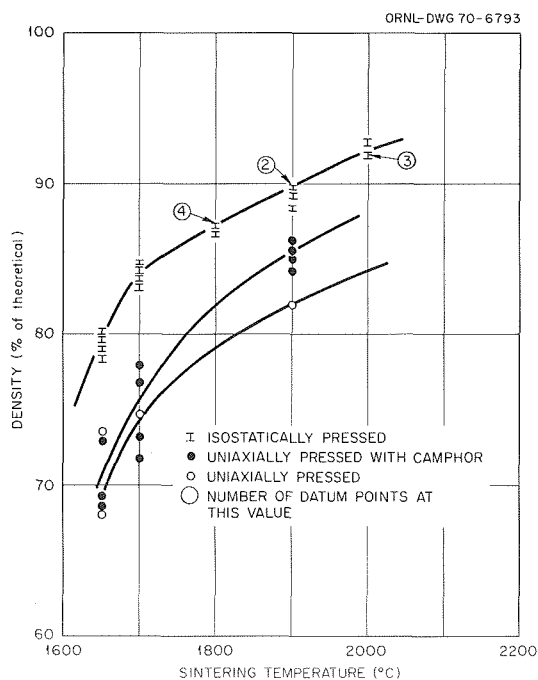


Fig. 22. Sintering Properties of UN Fabricated by Various Methods.

immersion method. The isostatically pressed specimens achieved the highest sintered densities. Considerable variation was observed in the densities of the uniaxially pressed specimens; a much smaller variation occurred in those pressed isostatically. The densities of the uniaxially pressed samples with and without camphor or a binder were similar.

THERMAL STABILITY OF UN

The stability of the microstructure and overall dimensions of UN when exposed to a high-temperature nonoxidizing atmosphere were investigated as a function of the specimen density at test conditions of 1400°C (1673 K) and 10 and 100 hr. A preliminary 10-hr experiment was conducted in order to evaluate the safety of the furnace equipment during the 100-hr experiment.

For the 10-hr test, three sets of UN pellets were fabricated by means of the process described in Fig. 12. They were sintered to bulk densities from 85 to 92% of theoretical. The microstructure of these pellets consisted of small grains (about 5 to 10 μm in diameter) with some interconnecting porosity. The samples were measured with a micrometer to ± 0.0002 in. ($\pm 5.08 \times 10^{-6}$ m) before and after the test.

The dimensions before and after the test along with the sintering conditions and densities for the individual specimens are given in Table 6.

Table 6. Effect of 10-hr Test at 1400°C (1673 K) on the Dimensions and Density of UN

Specimen ^a	Density, % of Theoretical		Diameter, in.		Length, in.	
	Initial ^b	Final ^c	Initial	Final	Initial	Final
R488-1	84.7	85.5	0.2700	0.2694	0.2590	0.2580
R487-2	87.3	87.2	0.2660	0.2655	0.2620	0.2618
R486-2	92.1	92.7	0.2610	0.2610	0.2530	0.2530

^aSintering Conditions for Test Specimens:

R488-1: 2 hr at 1650°C (1923 K) in 1 atm N₂ (1.01×10^5 N/m²).
 R487-2: 1 hr at 1700°C (1973 K) in 1 atm N₂ (1.01×10^5 N/m²).
 R486-2: 1 hr at 1900°C (2173 K) in 1 atm N₂ (1.01×10^5 N/m²).

^bInitial density = density determined before thermal test.

^cFinal density = density determined after 10 hr at 1400°C (1673 K) in vacuum.

Note that the nitride powder used for these specimens sintered to higher density at a given temperature than did that used for preparing the samples in the sintering study.

Figure 23 shows the microstructural changes observed as a result of the 10-hr test in our nitride specimen sintered to 85% of theoretical density. No significant changes were noted. Table 6 lists the specimen dimensions before and after the test. The dimensional changes were essentially within the range that could be read from the micrometer. Figures 23, 24, and 25 illustrate the microstructures of the specimens before and after the test. The 10-hr thermal test did not significantly change the microstructure or the dimensions of the specimens.

The specimens for the 100-hr test at 1400°C (1673 K) were sintered in the same way as part of those in the sintering study discussed previously and illustrated in Fig. 22. The isostatically pressed specimens and some of those fabricated with camphor were tested in the furnace with no encapsulation. All were weighed before and after the test to ± 0.0001 g ($\pm 10^{-7}$ kg).

The test furnace was controlled automatically at $1400 \pm 10^\circ\text{C}$ (1673 ± 12 K) during the entire 100-hr duration of the test, and the furnace pressure was maintained at 2 to 1×10^{-8} torr (2.66 to 1.33×10^{-6} N/m²) by means of an ion pump. The results of the measurements made on these specimens are given in Table 7. The measurements indicated no clear trend with respect to the original sintering temperature or fabrication technique. The specimens all exhibited very small weight loss, but the magnitude approximated the sensitivity of the analytical balance that was used. The dimensional changes are essentially within the limits of uncertainty of the micrometer measurements. The indicated changes in density appear to be random but may imply that a small increase in bulk density occurred due to the 100-hr exposure at 1400°C (1673 K). The density measurements clearly indicated a need for an improvement in the technique for measuring the bulk density of specimens that have volumes of 0.1 to 0.5 cm³.

The microstructures of the test specimens were examined; those of the isostatically pressed specimen sintered at 1700°C (1973 K) are shown

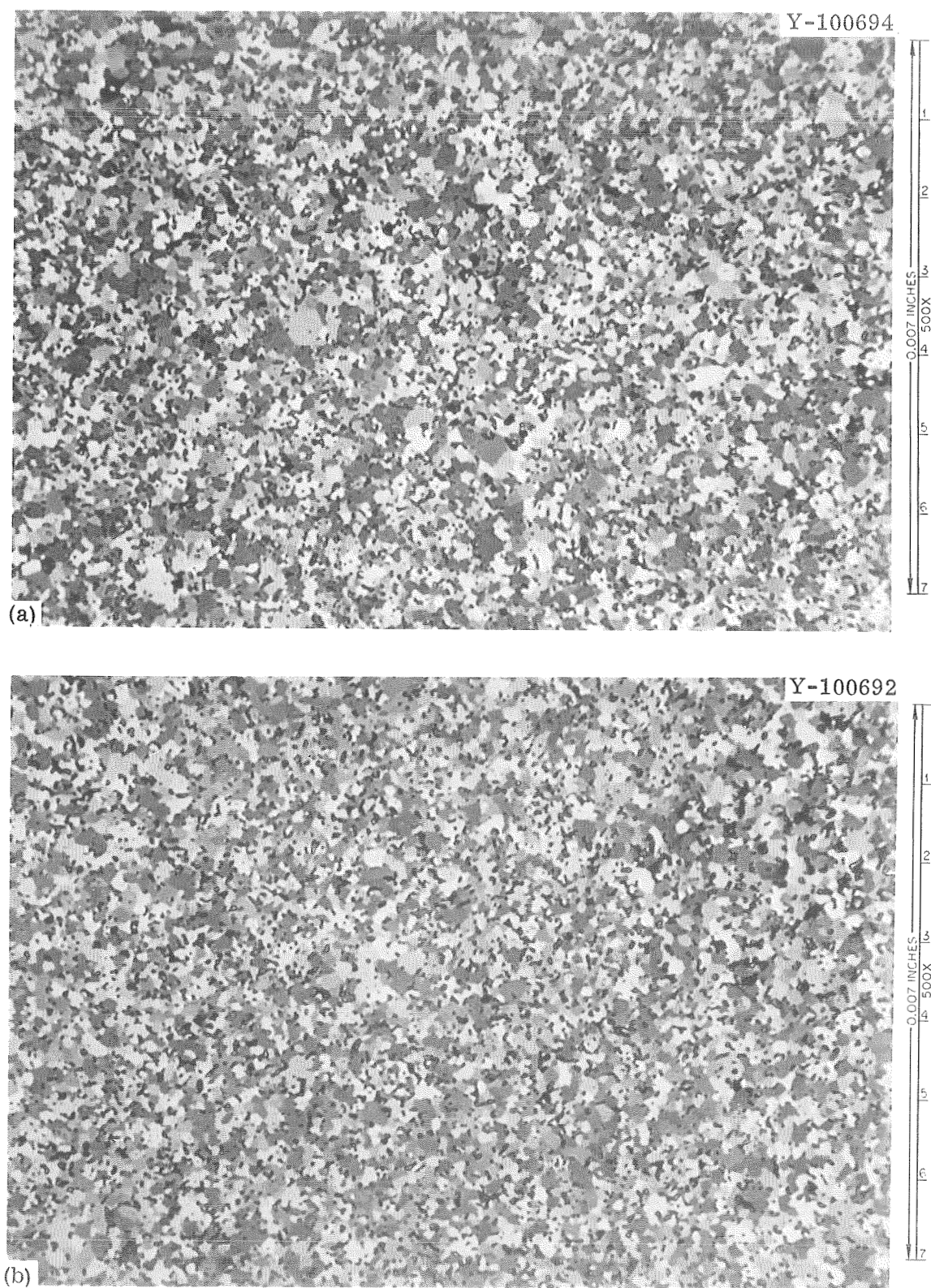


Fig. 23. Microstructures of UN (a) Specimen R488, Before Test and (b) Specimen R488-1, After Test.

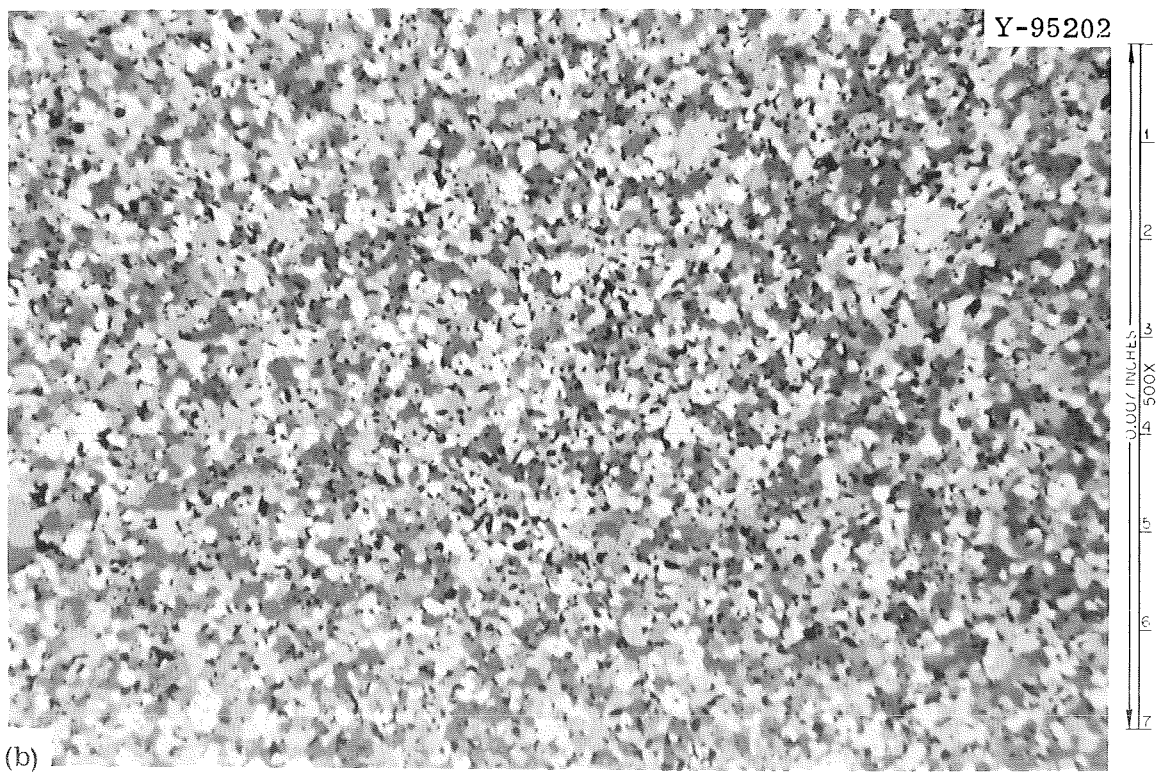
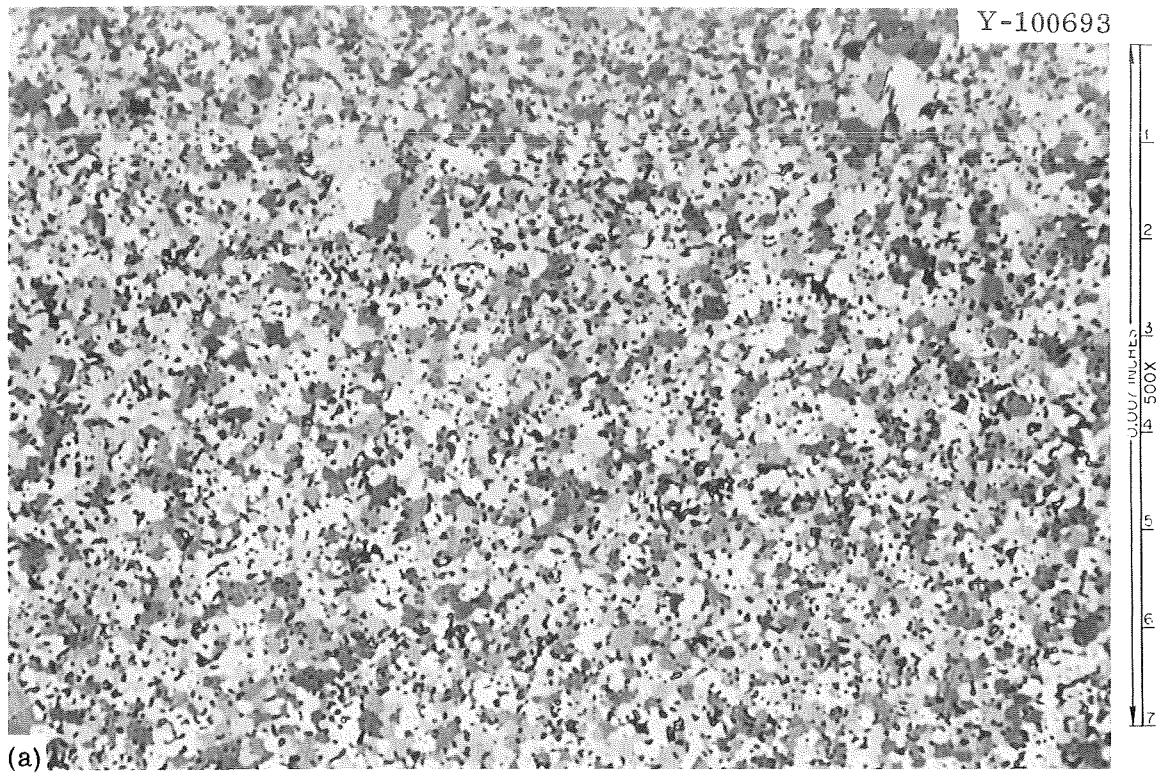


Fig. 24. Microstructures of UN (a) Specimen R487, Before Test and (b) Specimen R487-2, After Test.

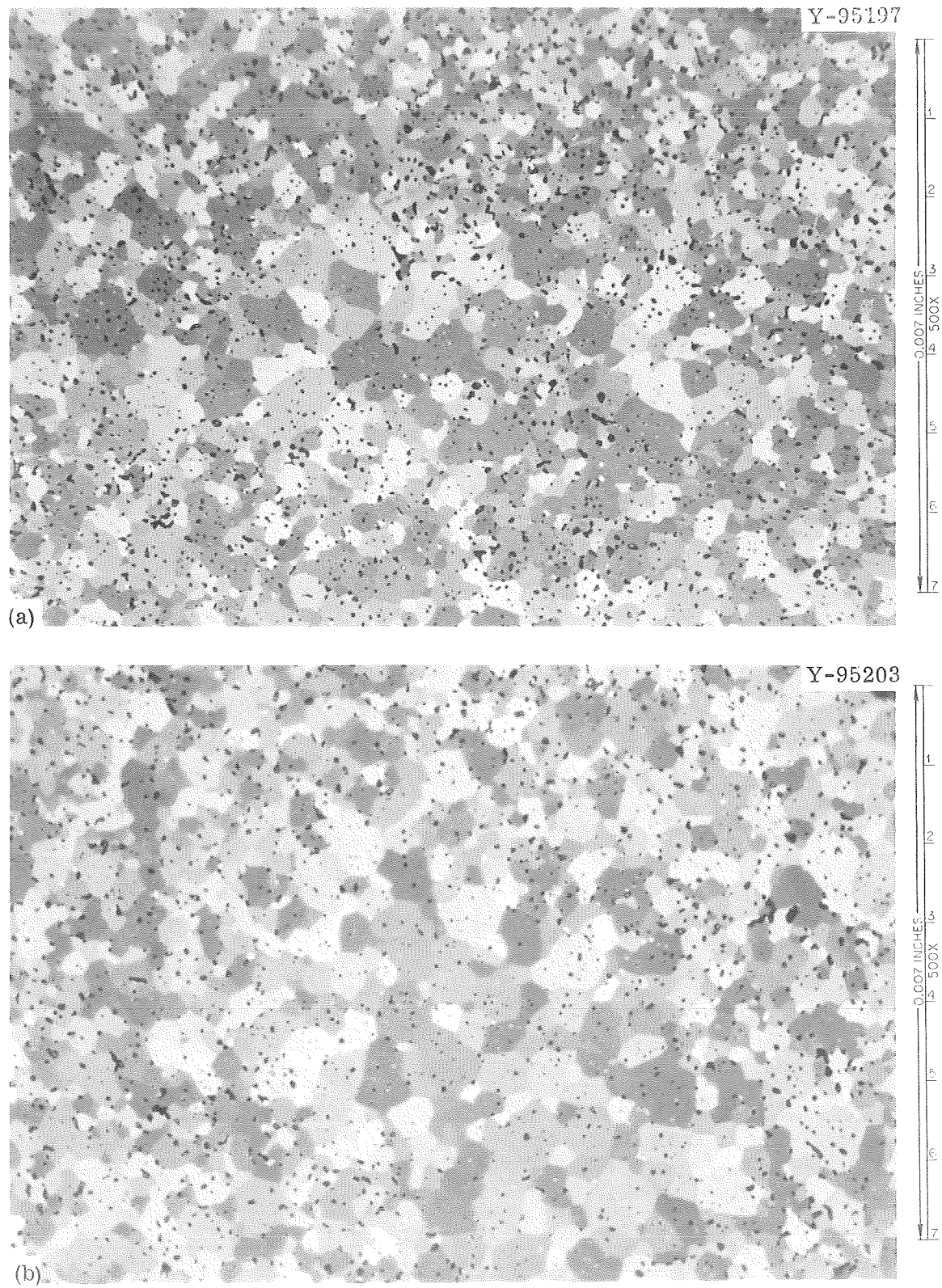


Fig. 25. Microstructures of UN (a) Specimen R486, Before Test and (b) Specimen R486-2, After Test.

Table 7. Results of Experiment on Microstructural Stability of UN
After 100 hr at 1400°C (1673 K) in Vacuum

Specimen	Immersion Density, % of Theoretical		Change in Density (%)	Average Shrinkage ^a (%)	Weight Loss (%)
	Initial	Final			
1650 ^b	78.4	80.2	2.3	1.1	0.08
1700 ^b	83.4	86.7	3.9	1.8	0.04
1800 ^b	87.1	90.5	3.9	1.9	0.05
1900 ^b	88.0	87.2	-1.0	0.3	0.07
2000 ^b	91.5	93.6	2.3	0.9	0.01
1700 ^c	77.4	74.4	-3.9	1.0	0.07
1900 ^c	84.9	85.6	0.8	0.3	0.08

^aAverage of length and diameter measurements on a given specimen.

^bIsostatically pressed specimen sintered for 1 hr in 1 atm N₂ (1.01×10^5 N/m²) at indicated temperature (°C).

^cUniaxially pressed specimen using binder (2% camphor in acetone) sintered for 1 hr in 1 atm N₂ (1.01×10^5 N/m²) at indicated temperature (°C).

in Fig. 26 before and after the test. This is the second specimen listed in Table 7. The grains in the untested specimen, IP-R5-17, shown in Fig. 26(a), were 3 to 6 μ m in diameter, and those in the tested specimen, shown in Fig. 26(b), were 7 to 10 μ m in diameter, indicating that some grain growth occurred. The microstructure of the uniaxially pressed specimen, UPNBR4-19, is shown in Fig. 27 before and after the test. This is the last specimen in Table 7. Initially the grains were 10 to 16 μ m in diameter, and those of the tested specimen were 10 to 18 μ m in diameter, indicating that the grains had grown very little if any as a result of the long-term heating. This result was probably because of the higher temperature of the initial sintering used to densify the uniaxially pressed specimen R4. The driving force for grain growth in R4 during the test was thus lower than it was in specimen R5.

No oxide phase or any second phase was observed at 500 \times in the specimens before or after either the 10- or 100-hr test. The

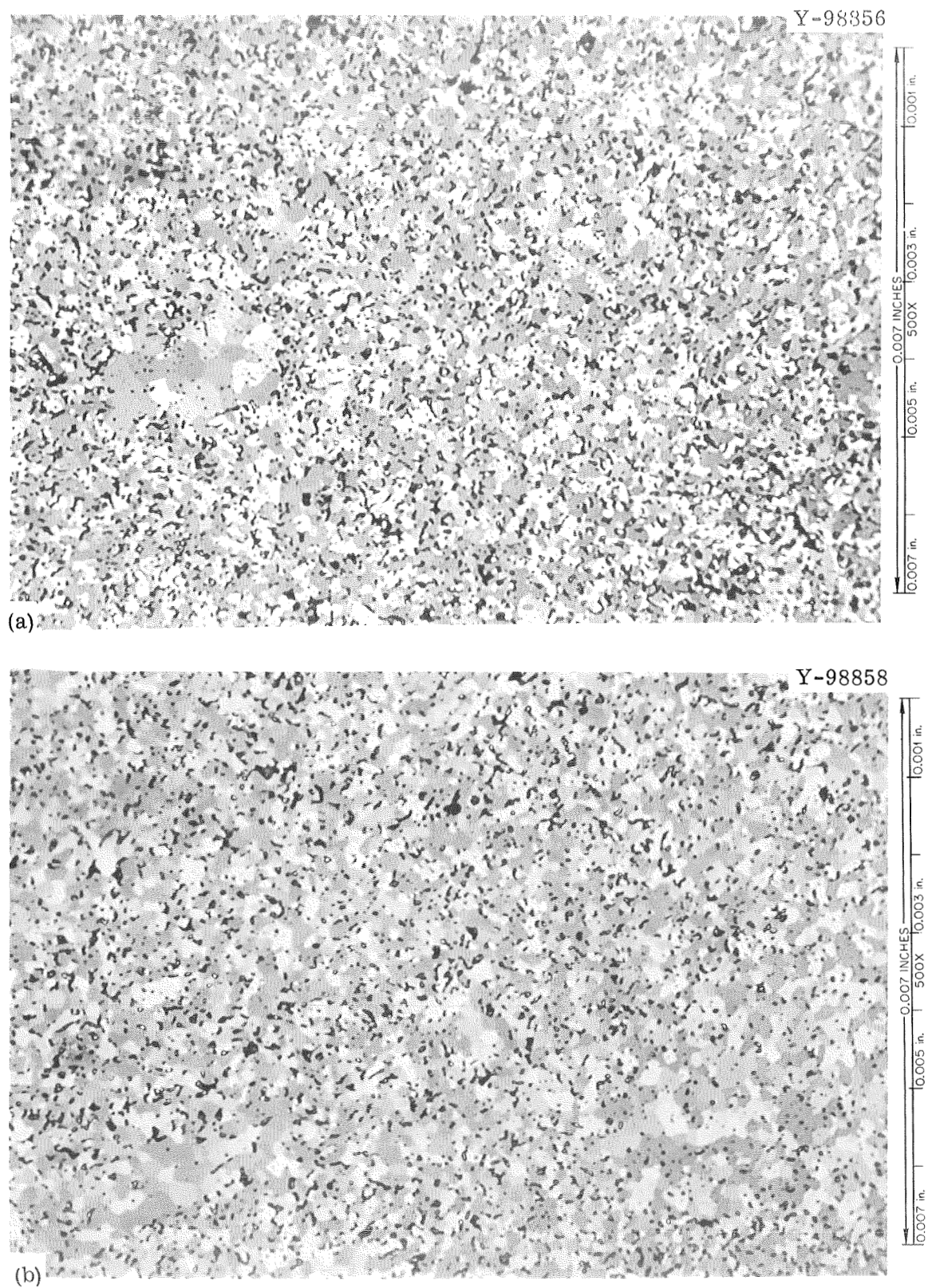


Fig. 26. Microstructure of Isopressed UN Specimen R5, Sintered at 1700°C. (a) Before test and (b) after test.

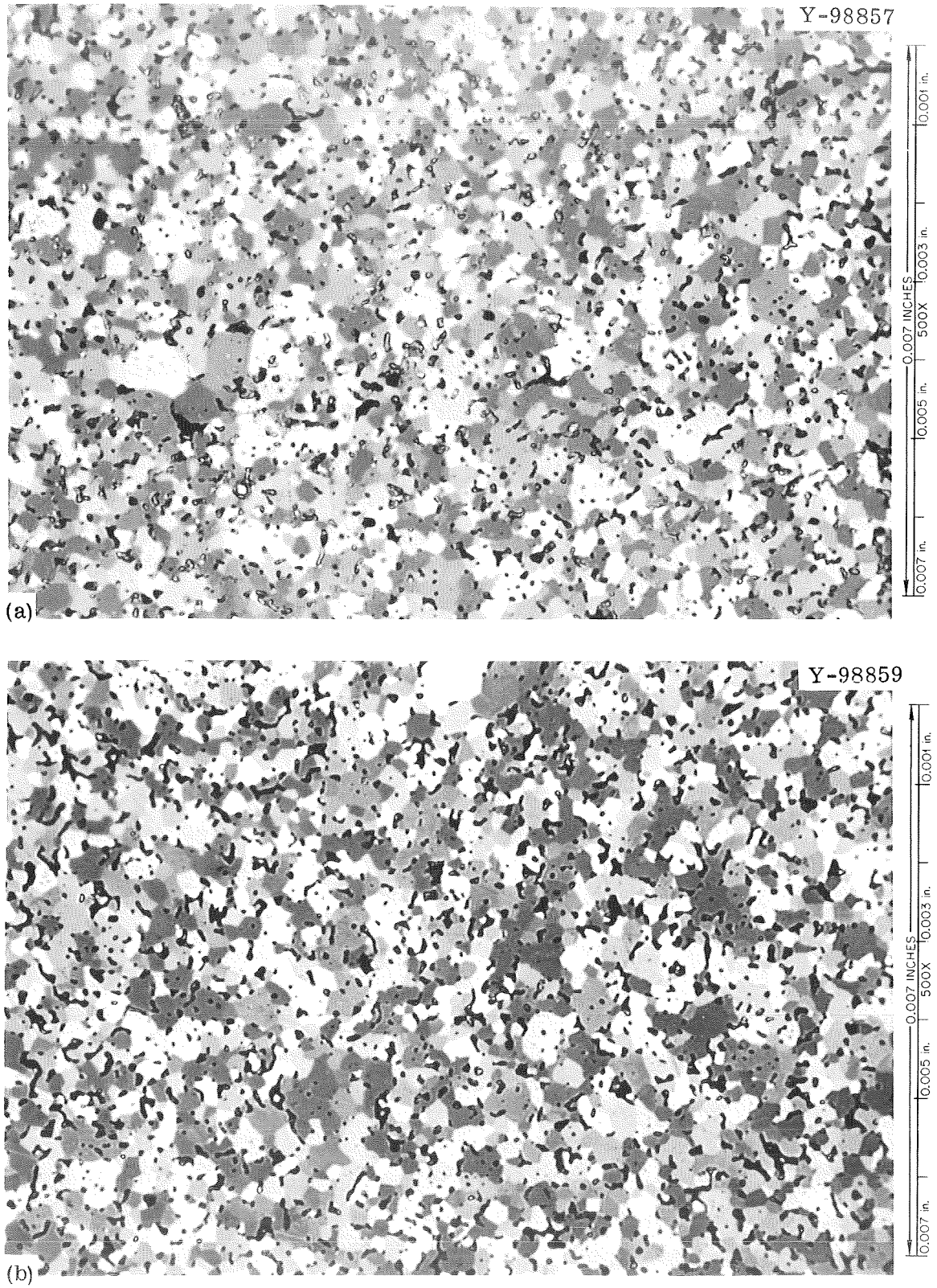


Fig. 27. Microstructure of Uniaxially Pressed UN Specimen R4, Sintered at 1900°C. (a) Before test and (b) after test.

isostatically pressed specimens contained about 500 ppm O after testing, whereas before test they contained about 350 ppm O.

The conclusions to be drawn from these tests are that UN that has a bulk density of about 85% of theoretical has reasonable dimensional stability at 1400°C (1673 K) for 100 hr. Linear shrinkages of 0.5 to 1% may be expected under these conditions.

MACHINING STUDY OF UN

During the course of this work several specimens of dense sintered UN were machined to dimensions with tolerances as small as ± 0.001 in. ($\pm 2.54 \times 10^{-5}$ m). Many of the specimens were solid cylinders with ratios of length to diameter near unity. Others were long cylinders of UN that had been fabricated by isostatic pressing and had ratios of length to diameter up to 5. Several problems were encountered in machining this material, and some of these will be reviewed qualitatively.

A cylindrical surface can most readily be ground on a preformed sintered cylinder of UN on a centerless grinder with water coolant. To date, the use of cylindrical grinding techniques with UN has been very unsuccessful. The centerless grinder, when set up properly, can remove a very small amount of the UN from the surface on each pass through the machine. The cylindrical grinder can, in principle, be adjusted to do the same. For the cylindrical grinder, however, a method must be provided for mounting the piece rigidly to the headstock. This is difficult with a very brittle material such as UN, and special training is required for the personnel who do the work. The brittleness appeared qualitatively to increase somewhat with the grain size as this varied in the range 10 to 60 μm in diameter.

The main problem observed with the centerless grinder was its tendency to "three-lobe" the cylinder and thus not to grind it in a perfect circle. This tendency was related to the precision and care with which the machine was adjusted and to the amount of material that had to be removed. If more than about 0.050 in. (12.7×10^{-4} m) was to be removed from the diameter of the cylinder, the three-lobing problem was usually encountered. Rigid, continuous inspection of the piece during this

entire operation was required. Wheels of medium hardness were usually most suitable for grinding UN.

The cylindrical grinding of annular cylinders with outside diameters of about 0.6 in. (1.52×10^{-2} m) and inside diameters of about 0.2 in. (0.508×10^{-2} m) was studied in some detail. The machining yield was no better than 15%; most of the cylinders were broken. An annular shape required that the cylinder be mounted on a mandrel, and no suitable technique was developed for rigidly mounting the heavy cylinders on such a small mandrel. During grinding, vibrations within the piece usually resulted in breakage. Many cylinders were broken while they were being mounted onto the mandrel.

The grinding of the end surfaces on both solid and annular cylinders was investigated in some detail. The two methods used involved (1) a grinding wheel mounted on a cylindrical grinder with the piece located in a rotating collet and (2) a conventional surface grinder, with the piece fastened to the bed of the machine. The use of a grinding wheel in a cylindrical grinder was found to be generally unsatisfactory. The mounting of the specimen in the collet often caused breakage of the piece, and the amount of cut employed on a pass with the wheel was difficult to keep low enough to avoid excessive heating and tearing of the specimen. In many cases, regions of the end surface of a cylinder would be torn out by this technique. It was also difficult to get the operator to make small enough cutting passes, since the time per pass was significant and the process was time consuming if large amounts of material were to be removed. The surface grinder was far superior for this purpose. A 100-grit silicon carbide wheel with a density of 5 in a scale of 14 was found to be very suitable for this work. The specimens were mounted in V-blocks to the bed of the grinder so that the end surface could be referenced to the cylindrical surface. Very small cuts could be made in a very controllable fashion.

Electrodischarge machining (EDM) methods for truing or dressing the annular holes in cylinders and for end facing small cylinders were investigated. This technique was very controllable and usually did not lead to breakage of the specimens but was very slow with the machine available.

To illustrate the observed effects, we prepared two isostatically pressed annular cylinders. One was sintered at 2000°C (2273 K) for 1 hr and the other at 2200°C (2473 K) for 1 hr to produce specimens with densities 88 to 91% of theoretical. The cylinders are shown in Fig. 28; specimen R16, sintered at 2200°C (2473 K), is shown on the right, and specimen R17, sintered at 2000°C (2273 K), is on the left. The cylindrical surfaces of the cylinders were ground on the centerless grinder, and the annular holes were machined to size by the EDM method.

The microstructure of the interior of specimen R16 is shown in Fig. 29(a). This section was taken about 0.020 in. (5.08×10^{-4} m) from the end of the sintered piece. The grains were about 10 to 20 μm in diameter. The microstructure of specimen R17 is shown in Fig. 29(b). The grains in this specimen were about 10 μm in diameter due to the lower sintering temperature employed for R17.

Part of the free surface of the inner surface of R17 is shown in Fig. 30. This surface had a feathery character and considerable open porosity near the surface was indicated by the penetration of the

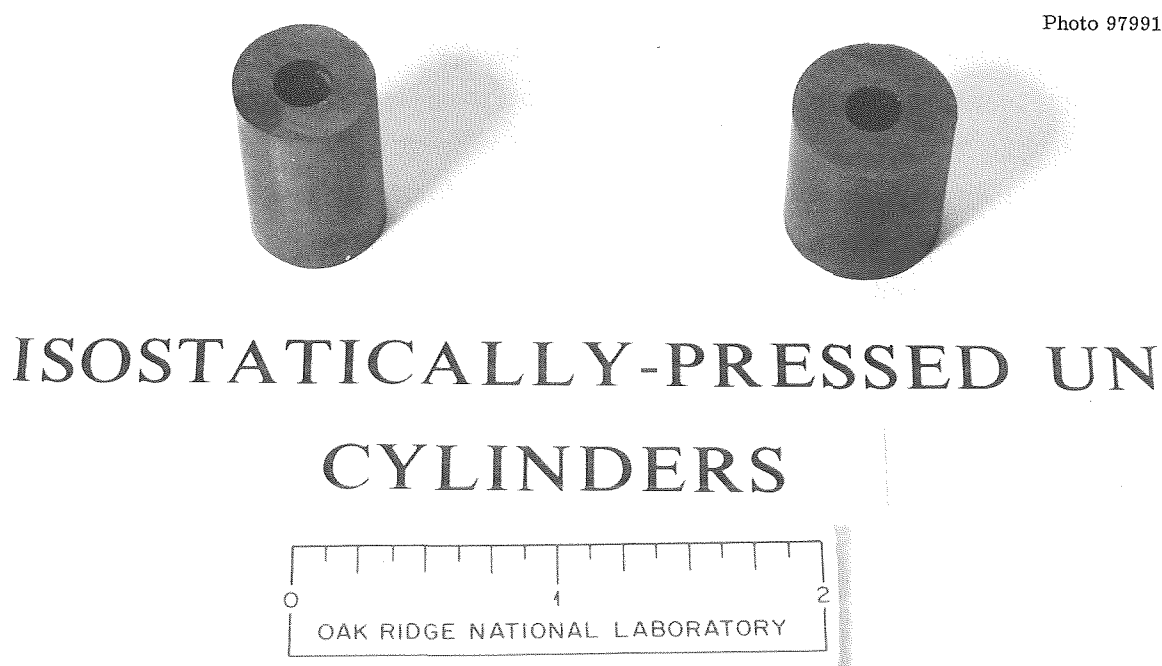


Fig. 28. Typical UN Cylinders Used in Machining Experiments.

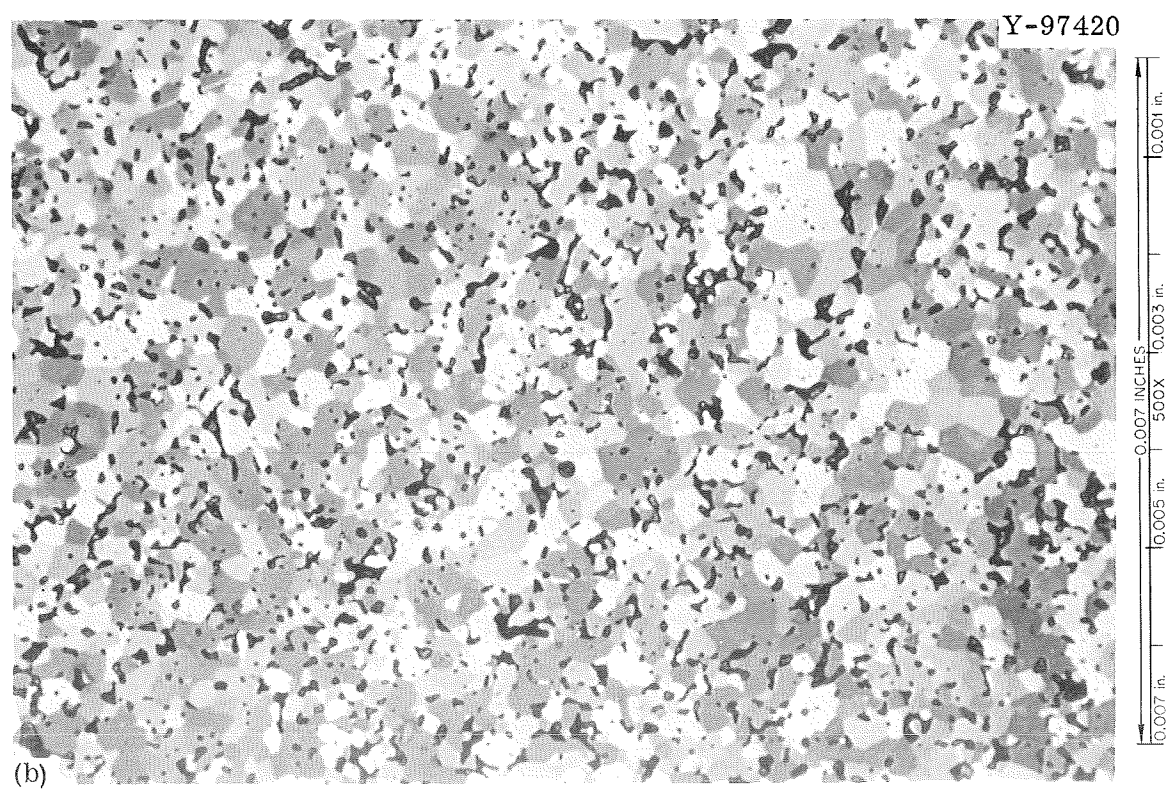
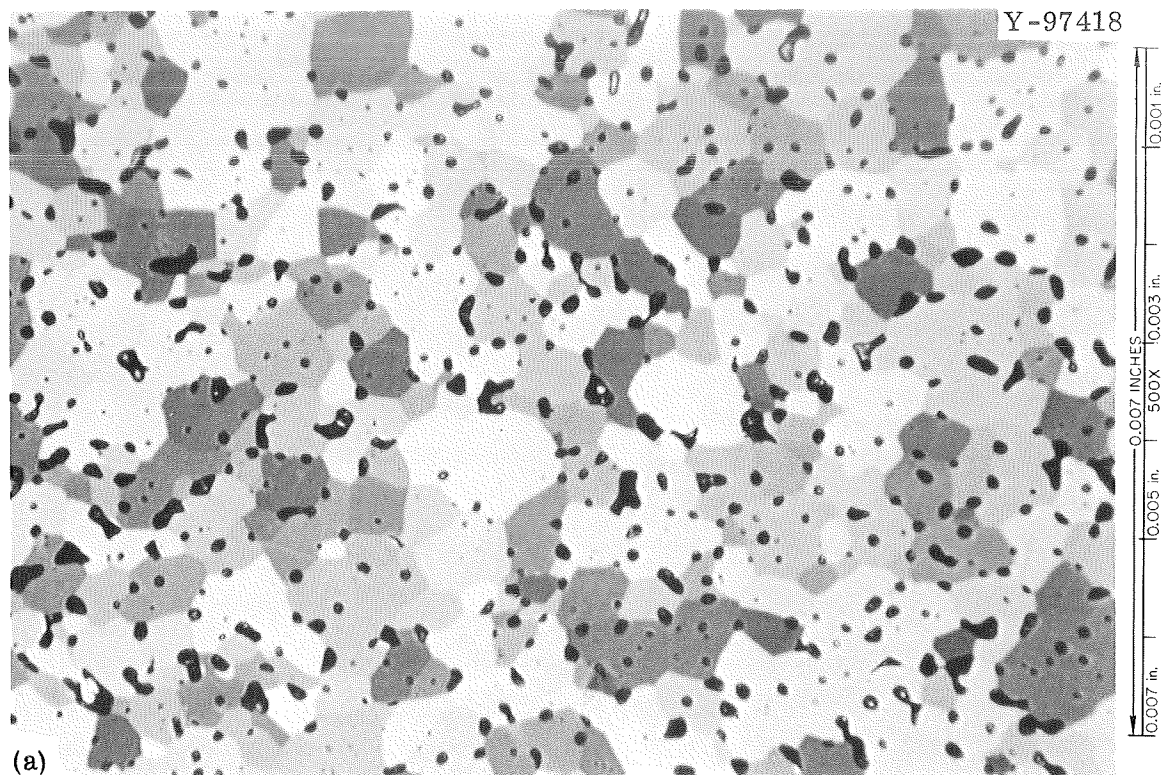


Fig. 29. Microstructure of UN Specimens. (a) R16, 91% of theoretical density and (b) R17, 88% of theoretical density.

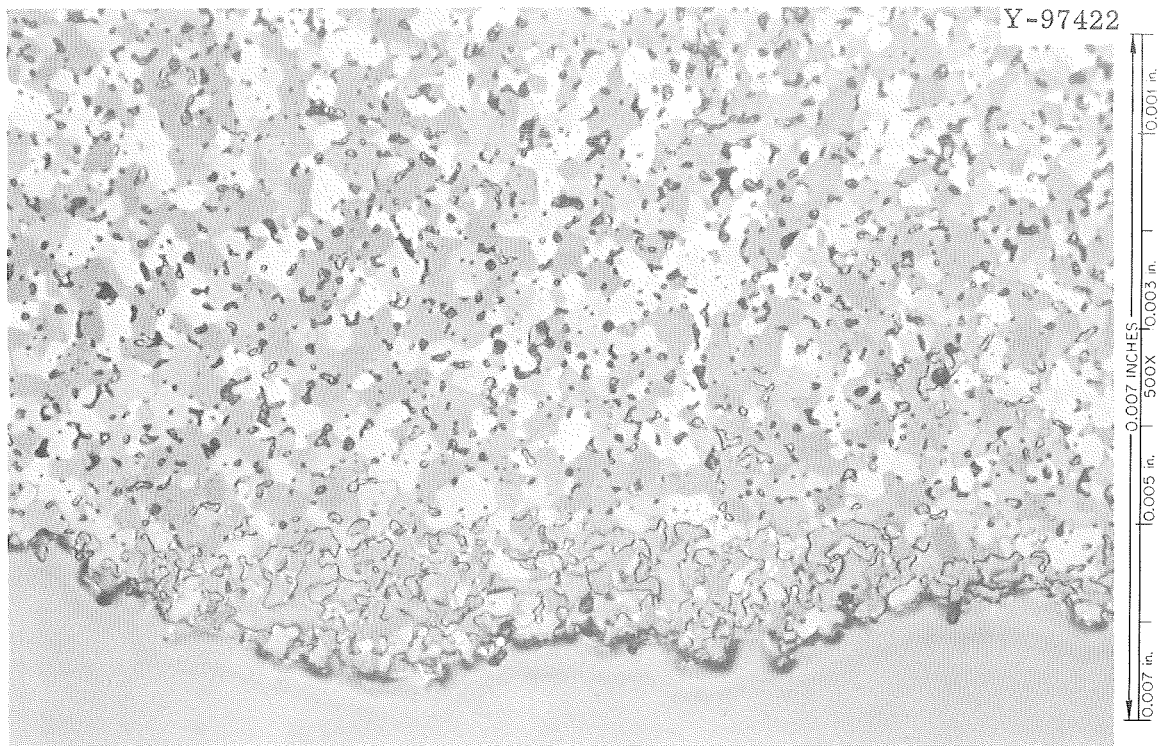


Fig. 30. Microstructure of Unmachined Inner Surface of UN Specimen R17.

Araldite impregnant into the surface for a distance of about $40\text{ }\mu\text{m}$. A portion of the inner surface of R17 after machining by EDM is shown in Fig. 31(a). Note the smoothness of the surface and the thin layer of a bright, globular phase on the surface. This phase apparently originated from the use of EDM procedures. The phase was not identified. Since the Araldite penetrated about 40 to $50\text{ }\mu\text{m}$ in this region, the EDM technique did not cause a closing off of the pore phase at the surface.

The ground surface of R17 is shown in Fig. 31(b). Again, the mounting material penetrated about $40\text{ }\mu\text{m}$. The ground surface contained several microcracks that presumably are due to the stresses imposed during grinding.

The results for R16 were essentially identical, except that much less of the mounting material penetrated the specimen due to its lower open porosity. Examination of these microstructures did not reveal any significant amount of abrasive grain that had penetrated the open porosity

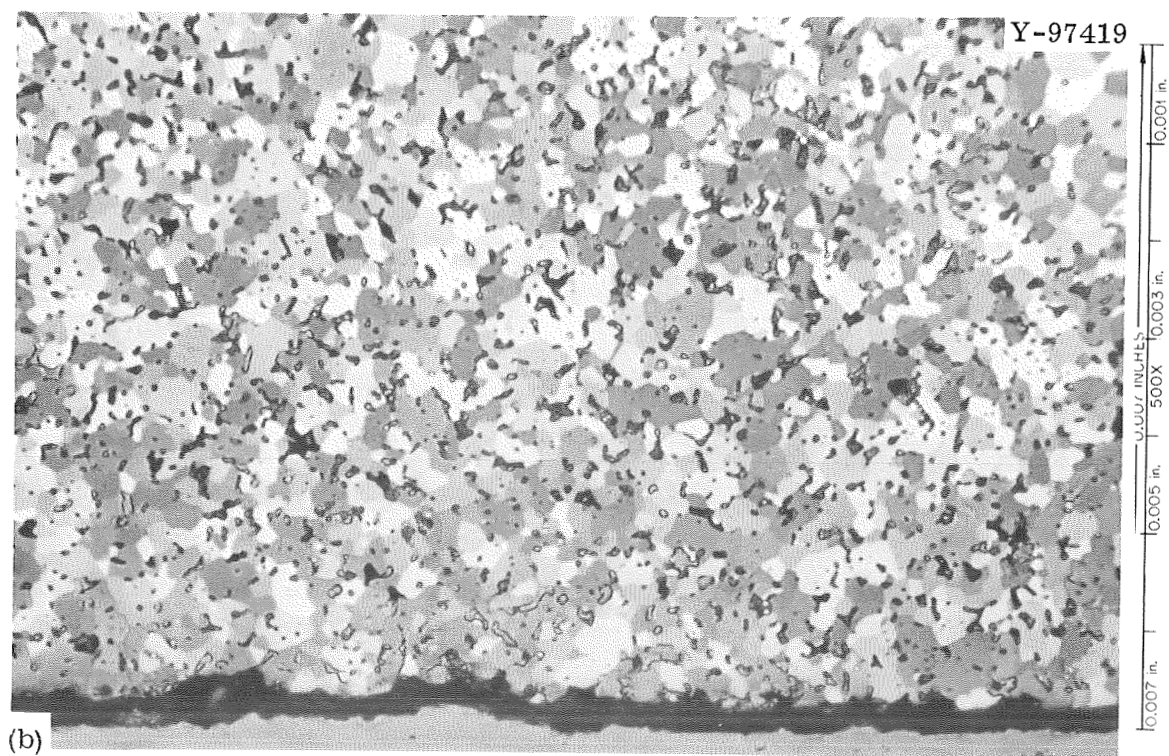
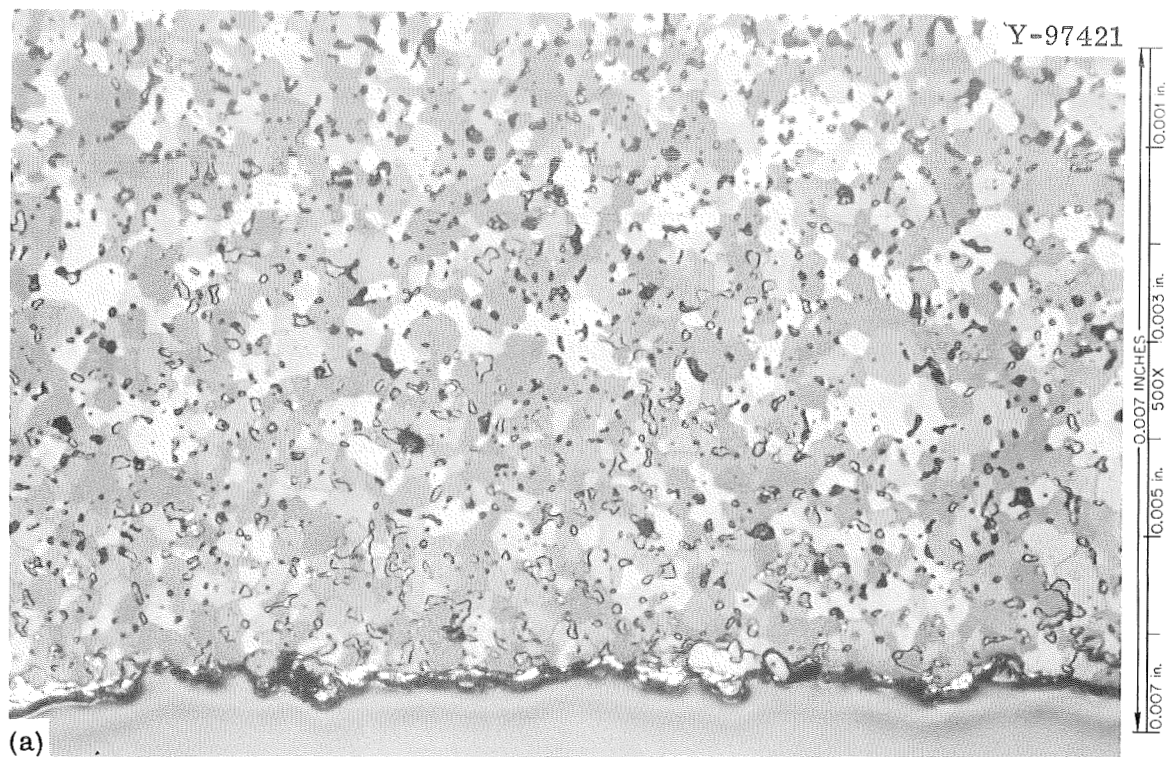


Fig. 31. Microstructure of UN Specimen R17. (a) Inner surface, machined by electrodischarge machining and (b) outer surface, ground on a centerless grinder.

during the machining procedures. The pores were small, and penetration by the relatively coarse abrasive was apparently difficult.

UN SPECIMENS DELIVERED TO THE LEWIS RESEARCH CENTER OF THE NATIONAL AERONAUTICS AND SPACE ADMINISTRATION

During the course of this work, several different specimens of sintered UN were delivered to NASA-Lewis for reactor loop tests and for experiments on its compatibility with lithium. One group of specimens for loop tests was solid cylinders 0.658 in. in diameter (1.67×10^{-2} m) by 0.412 in. long (1.05×10^{-2} m) with tolerances of ± 0.001 in. ($\pm 2.54 \times 10^{-5}$ m). These specimens had densities from 93.6 to 94.5% of theoretical, and the chemical analysis of control specimens for the three sintering runs used to produce the cylinders gave the results shown in Table 8. The specimens were uniaxially pressed with camphor

Table 8. Chemical Analyses of Sintering Control Specimens

Sintering Run	Composition, %			
	U	N	C	O
479	94.47	5.32	0.033	0.15
481	94.56	5.31	0.029	0.15
483	94.23	5.27	0.076	0.23

as a binder and lubricant at 10,000 psi (6.89×10^7 N/m²) and then isostatically pressed at 50,000 psi (34.5×10^7 N/m²). These specimens represented a total mass of 500 g of machined parts of UN.

Because of concern about the role of oxygen in single phase UN in reactions with lithium, we fabricated and sintered five large cylinders to have very low oxygen contents. Five specimens of about 80 g each were isostatically pressed and sintered so that the outside diameter could be machined to 0.658 in. (1.67×10^{-2} m) and the length to 0.825 in. (2.10×10^{-2} m). The cylinders were about 93.5% of theoretical density. The oxygen analyses of a control specimen for sintering run V-6 indicated 150, 190, and 200 ppm O in a triplicate analysis. The

microstructure of this material is shown in Fig. 32. These specimens represented a total of 411 g of UN.

Two sets of specimens were provided to NASA-Lewis for use in experiments on compatibility with lithium. The first set consisted of rods of sintered UN that had three different oxygen contents. The designations for these specimens and their analyzed oxygen contents were low oxygen (250 to 300 ppm O), intermediate oxygen (750 to 800 ppm O), and high oxygen (1850 to 2000 ppm O). These rods consisted of a total mass of 48 g of UN. The second set of UN rods consisted of 15 isostatically pressed specimens that were sintered in runs V-8, -11, and -12. The oxygen contents obtained for each set were as follows:

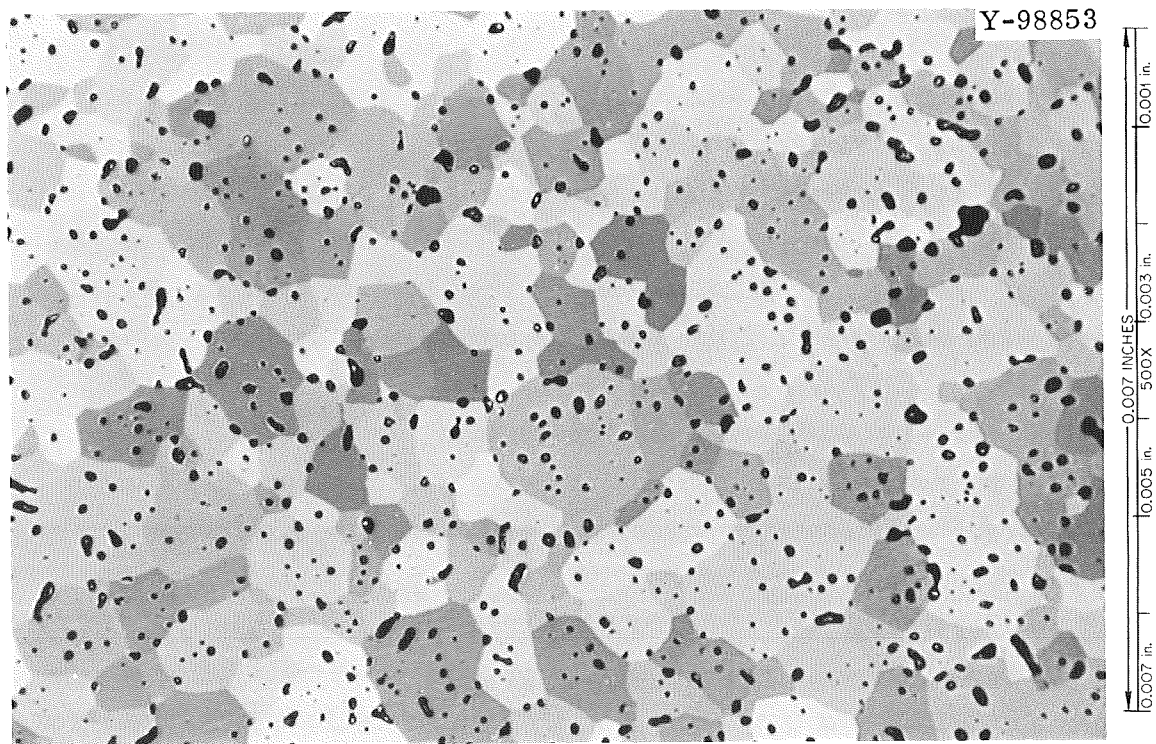


Fig. 32. Microstructure of a UN Specimen from Sintering Run V-6 for Loop Test of Compatibility with Lithium.

<u>Sintering Run</u>	<u>Oxygen Content, ppm</u>
V-8	{ 370 430 380
V-11	{ 130 110
V-12	{ 140 110

Microstructures typical of runs V-8 and V-11 are shown in Fig. 33. These rods had densities of about 93.6% of theoretical, and the total mass was 360.1 g.

CONCLUSIONS

Uranium nitride powders made from the metal by the hydride-dehydride-nitride synthesis process were characterized by measuring the distributions of particle sizes and examining the particles by scanning electron microscopy. The average particle was about 2 to 5 μm in diameter, and the particles were irregularly shaped. Careful control of the oxygen content of the gases used in the process resulted in uranium nitride powders with as low as 100 ppm O, as determined by the inert-gas-fusion method.

The nitride powders were fabricated into useful shapes such as cylinders by two methods, uniaxial pressing with camphor as a binder and lubricant and isostatic pressing with no additives. Isostatic pressing was superior, for cylinders with large ratios of length to diameter could be fabricated, and sintered UN fabricated by this process had less than 300 ppm O, whereas the uniaxially pressed material typically contained about 1000 ppm O or more. Large annular cylinders that weighed 140 g or more were fabricated by isostatic pressing while maintaining good dimensional control of the outside diameter, the inside diameter, the length, and the concentricity of the inner hole.

Problems associated with adequate quantitative analysis of UN are the precision and accuracy of the uranium and nitrogen determinations. Precision of at least 1 part in 5000 would be desirable for the uranium

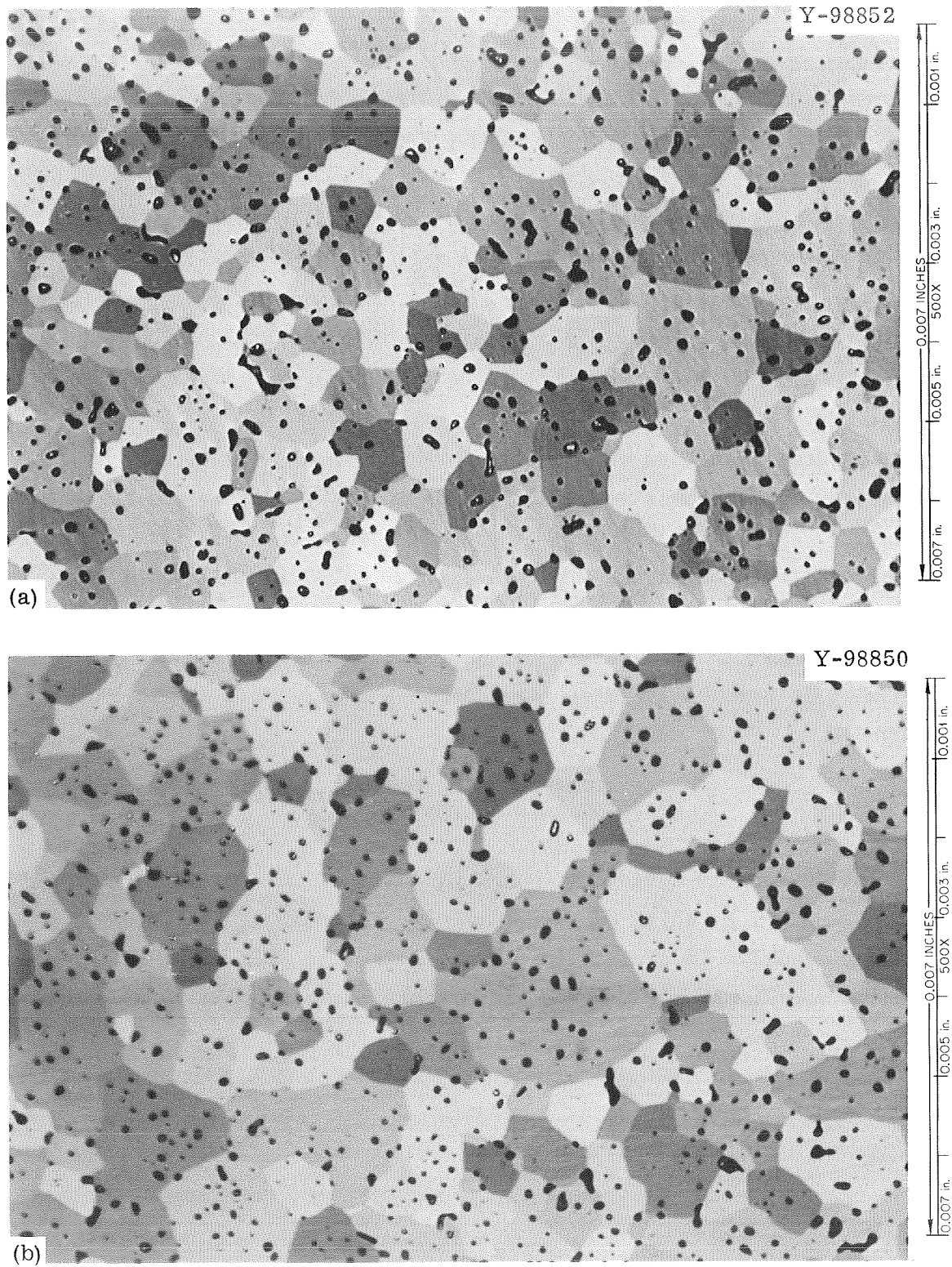


Fig. 33. Microstructures of UN Specimens for Tests of Compatibility with Lithium. (a) Sintering run V-8 and (b) sintering run V-11.

determination, and precision of 1 part in 500 or better is needed for the nitrogen determination.

Uranium nitride sinters appreciably at temperatures above 1700°C (1973 K) in 1 atm N₂ (1.01×10^5 N/m²). Densities above 93% of theoretical could be achieved only at temperatures of 2300°C (2573 K) and above. Appreciable congruent evaporation of the UN occurs at temperatures above 2350°C (2623 K) at 1 atm N₂ (1.01×10^5 N/m²).

The microstructure and dimensions of 85% dense UN are essentially unchanged by heat treating in vacuum at 1400°C (1673 K) for periods of up to 100 hr. A small amount of grain growth occurs under these conditions.

The brittle nature of dense sintered UN makes it difficult to machine by conventional grinding methods without chipping and breakage occurring. When sintered UN 85 to 95% of theoretical density is properly supported it can be machined successfully. Grinding on a centerless grinder is easier than cylindrical grinding. Specimens can be machined by EDM with little difficulty, but the time required for this type of machining is prohibitive when large amounts of material are to be removed.

ACKNOWLEDGMENTS

The invaluable assistance of J. L. Botts of the Analytical Chemistry Division and M. D. Allen of the Metallography Group of the Metals and Ceramics Division is gratefully appreciated. The work of J. E. Pope and T. W. Coffey of the Ceramics Laboratory was essential to this program.

NASA DISTRIBUTION

Robert R. Metroka (61)	NASA Lewis Research Center 21000 Brookpark Road Cleveland, Ohio 44135
Leonard Schopen (1)	NASA Lewis Research Center 21000 Brookpark Road Cleveland, Ohio 44135
Neal T. Saunders (1)	NASA Lewis Research Center 21000 Brookpark Road Cleveland, Ohio 44135
Samuel J. Kaufman (1)	NASA Lewis Research Center 21000 Brookpark Road Cleveland, Ohio 44135
Richard Gluyas (1)	NASA Lewis Research Center 21000 Brookpark Road Cleveland, Ohio 44135
Armin Lietzke (1)	NASA Lewis Research Center 21000 Brookpark Road Cleveland, Ohio 44135
Morton Krasner (1)	NASA Lewis Research Center 21000 Brookpark Road Cleveland, Ohio 44135
Lewis Library (2)	NASA Lewis Research Center 21000 Brookpark Road Cleveland, Ohio 44135
Lewis Technical Information Center (1)	NASA Lewis Research Center 21000 Brookpark Road Cleveland, Ohio 44135
Mervin Ault (1)	NASA Lewis Research Center 21000 Brookpark Road Cleveland, Ohio 44135
NASA Lewis Report Control (1)	NASA Lewis Research Center 21000 Brookpark Road Cleveland, Ohio 44135
Ralph Stein (1)	NASA Lewis Research Center Plum Brook Station Standusky, Ohio 44870

NASA Headquarters Technical Information Abstracting and Dissemination Facility (6)	NASA Scientific and Technical Information Facility Box 5700 Bethesda, Maryland Att: NASA Representative
George Deutsch RR-1 (1)	NASA Headquarters Washington, D. C. 20546
Jim Lynch RNP (1)	NASA Headquarters Washington, D. C. 20546
Lewis Office of Reliability and Quality Assurance (1)	NASA Lewis Research Center 21000 Brookpark Road Cleveland, Ohio 44135 Att: Office of Reliability and Quality Assurance
Ames Research Center (1)	NASA Ames Research Center Moffett Field, California 94035 Att: Library
Flight Research Center (1)	NASA Flight Research Center P. O. Box 273 Edwards, California 93523 Att: Library
Goddard Space Flight Center (1)	NASA Goddard Space Flight Center Greenbelt, Maryland 20771 Att: Library
Jet Propulsion Laboratory (1)	Jet Propulsion Laboratory 4800 Oak Grove Drive Pasadena, California 91103 Att: Library
Langley Research Center (1)	NASA Langley Research Center Langley Station Hampton, Virginia 23365 Att: Library
Manned Spacecraft Center (1)	NASA Manned Spacecraft Center Houston, Texas 77001 Att: Library
Marshall Space Flight Center (1)	NASA Marshall Space Flight Center Huntsville, Alabama 35812 Att: Library
Western Operations (1)	NASA Western Operations 150 Pico Blvd. Santa Monica, California 90406 Att: Library

Ron Anderson RDT-USAEC (1)	U.S. Atomic Energy Commission Division of Reactor Development and Technology Fuels and Material Branch Washington, D. C. 20545
Jules Simmons RDT-USAEC (1)	U.S. Atomic Energy Commission Division of Reactor Development and Technology Fuels and Material Branch Washington, D. C. 20545
Don deHalas (1)	Battelle Northwest Laboratory 1112 Lee Boulevard P. O. Box 999 Richland, Washington 99352
Don Keller (1)	Battelle - Columbus 505 King Ave. Columbus, Ohio 43201
Ben Vondra (1)	Nuclear Material and Equipment Corp. 609 North Warren Avenue Appollo, Pennsylvania 15613
Jim Kane (1)	Lawrence Radiation Laboratory Atomic Energy Commission University of California P. O. Box 8081 Livermore, California 94551
AI - Library (1)	Atomic International North American Aviation P. O. Box 309 8900 DeSoto Ave. Canoga Park, California 91304
Warren Phillips (1)	Jet Propulsion Laboratory 4800 Oak Grove Dr. Pasadena, California 91103
United Nuclear - Library (1)	United Nuclear Grossland Road Elmsford, New York 10523
Clay Brassfield (1)	General Electric Co. P. O. Box 15132 Cincinnati, Ohio 45215

ORNL-4608
UC-25 - Metals, Ceramics, and Materials

AEC DISTRIBUTION

INTERNAL DISTRIBUTION

- | | |
|-------------------------------------|-----------------------------------|
| 1-3. Central Research Library | 60. W. J. Lackey |
| 4. ORNL - Y-12 Technical Library | 61. J. M. Leitnaker |
| Document Reference Section | 62. T. B. Lindemer |
| 5-24. Laboratory Records Department | 63. E. L. Long, Jr. |
| 25. Laboratory Records, ORNL RC | 64. A. L. Lotts |
| 26. ORNL Patent Office | 65. T. S. Lundy |
| 27. G. M. Adamson, Jr. | 66. E. J. Manthos |
| 28. E. S. Bomar, Jr. | 67. H. E. McCoy, Jr. |
| 29. R. A. Bradley | 68. D. L. McElroy |
| 30. J. H. Coobs | 69. J. L. Miller, Jr. |
| 31. W. H. Cook | 70. C. S. Morgan |
| 32. G. L. Copeland | 71. P. Patriarca |
| 33. C. M. Cox | 72. W. H. Pechin |
| 34. F. L. Culler | 73. C. B. Pollock |
| 35. D. R. Cuneo | 74-78. R. A. Potter |
| 36. J. E. Cunningham | 79. J M Robbins |
| 37. J. P. De Luca | 80. C. F. Sanders |
| 38. J. H. DeVan | 81. A. C. Schaffhauser |
| 39. R. G. Donnelly | 82. J. D. Sease |
| 40. W. P. Eatherly | 83. J. L. Scott |
| 41. J. I. Federer | 84. D. A. Sundberg |
| 42. R. B. Fitts | 85-89. V. J. Tennery |
| 43. J. H. Frye, Jr. | 90. D. B. Trauger |
| 44. W. Fulkerson | 91. T. N. Washburn |
| 45. F. J. Furman | 92. S. C. Weaver |
| 46-50. T. G. Godfrey | 93. A. M. Weinberg |
| 51. R. J. Gray | 94. J. R. Weir, Jr. |
| 52. R. L. Hamner | 95. R. K. Williams |
| 53. W. O. Harms | 96. C. S. Yust |
| 54. R. F. Hibbs | 97. C. M. Adams, Jr. (Consultant) |
| 55-57. M. R. Hill | 98. Leo Brewer (Consultant) |
| 58. C. R. Kennedy | 99. L. S. Darken (Consultant) |
| 59. T. G. Kollie | 100. Walter Kohn (Consultant) |

EXTERNAL DISTRIBUTION

101. D. F. Cope, RDT, SSR, AEC, Oak Ridge National Laboratory
102. C. L. Matthews, RDT, OSR, AEC, Oak Ridge National Laboratory
103. J. M. Simmons, Division of Reactor Development and Technology,
AEC, Washington

- 104. E. E. Stansbury, the University of Tennessee
- 105. J. A. Swartout, Union Carbide Corporation, New York
- 106. Laboratory and University Division, AEC, Oak Ridge Operations
- 107. Patent Office, AEC, Oak Ridge Operations
- 108-306. Given distribution as shown in TID-4500 under Metals, Ceramics,
and Materials category (25 copies - NTIS)